The roles of HOXD10 in the development and progression of head and neck squamous cell carcinoma (HNSCC)

Fahad Hakami[1, 2], Lav Darda[1], Prachi Stafford[1], Penella Woll[3], Daniel W Lambert[1], Keith D Hunter[1, 4]

[1]Unit of Oral & Maxillofacial Pathology, School of Clinical Dentistry, University of Sheffield, Sheffield, S10 2TA, UK

[2]Department of Pathology and Laboratory Medicine, King Abdulaziz Medical City-WR, Jeddah, Saudi Arabia

[3]Academic Unit of Clinical Oncology, University of Sheffield, Sheffield, S10 2SJ, UK

[4]Department of Oral Pathology and Biology, University of Pretoria, Pretoria, South Africa

Address for Correspondence

Dr Keith D Hunter
Unit of Oral and Maxillofacial Pathology
School of Clinical Dentistry
University of Sheffield
Claremont Crescent
Sheffield
S10 2TA
UK
Email: k.hunter@sheffield.ac.uk
Fax: 0114 271 7894

Abstract

Background: HOX gene expression is altered in many cancers; previous microarray revealed changes in HOX gene expression in HNSCC, particularly HOXD10. **Methods:** HOXD10 expression was assessed by qPCR and immunoblotting in vitro and by IHC in tissues. Low-expressing cells were stably transfected with HOXD10 and the phenotype assessed by MTS, migration and adhesion assays and compared with the effects of siRNA knockdown in high HOXD10 expressing cells. Novel HOXD10 targets were identified using expression microarrays, confirmed by reporter assay, and validated in tissues by IHC. **Results:** HOXD10 expression was low in NOKs, high in most primary tumour cells, and low in lymph node metastasis cells, a pattern confirmed by IHC in tissues. Over-expression of HOXD10 decreased cell invasion but increased proliferation, adhesion and migration, with knock-down causing reciprocal effects. There was no consistent effect on apoptosis. Microarray analysis identified several putative HOXD10-responsive genes, including angiomotin (AMOT-p80) and miR146a. These were confirmed as HOXD10 targets by reporter assay. Manipulation of AMOT-p80 expression resulted in phenotypic changes similar to those on manipulation of HOXD10 expression. **Conclusion:** HOXD10 expression varies by stage of disease and produces differential effects; high expression giving cancer cells a proliferative and migratory advantage, and low expression may support invasion/metastasis, in part by modulating AMOT-p80 levels.

Keywords:

HOX genes, HOXD10, HNSCC, cancer, head & neck, tumour, metastasis, transcription factor, AMOT-p80, miR146a.

Introduction

Alterations in the genome and transcriptome of head and neck squamous cell carcinoma (HNSCC) are variable and related to the cancer site and stage. This heterogeneity has hindered the identification of molecular alterations that could be exploited as therapeutic targets in HNSCC. The prognosis for patients with HNSCC remains poor for the majority of patients who present at an advanced stage of disease (Leemans *et al*, 2011). Recent advances in the genomic characterisation of HNSCC have identified a number of potential somatic drivers, including NOTCH, but these are not ubiquitous and sub-classification of HNSCC will be required as further detail emerges (Agrawal *et al*, 2011; Pickering *et al*, 2013). It is not yet known whether alterations in these newly identified oncogenic drivers are related to disease severity or clinical outcome in HNSCC.

Our previous transcriptomic analysis of cell cultures from all stages of HNSCC development identified consistent alterations including dysregulation of expression of a number of HOX genes (Hunter *et al*, 2006), one of which was HOXD10. HOX genes form a large group of 39 homeodomain-containing transcription factors, found within 4 clusters in the genome (A, B, C and D), which are involved in embryonic development and also have a role in stem cell function (Picchi *et al*, 2013). Alterations in expression of HOX genes have been identified in a number of cancers, including haematolymphoid/leukaemias, breast and lung cancer (Abe *et al*, 2006; Gilbert *et al*, 2010; Rice & Licht, 2007).

Given their wide range of functions, it is not surprising that HOX genes may be either silenced or over-expressed in cancer. The effects of this aberrant expression in tumour cells include alterations in differentiation, apoptosis and receptor signalling pathways, and have been associated with control of EMT and promotion or inhibition of invasion (Wardwell-Ozgo *et al*, 2013; Wu *et al*, 2006). Control of expression is complex and for many HOX genes, has not been fully elucidated, however, epigenetic control and the action of microRNAs and other non-coding RNAs, such as HOTAIR, have been demonstrated (Rinn *et al*, 2007). Furthermore, the similarity in function between the paralogous groups of HOX genes introduces an element of functional redundancy, yet it is clear that the functions are not completely interchangeable between paralogues (Eklund, 2007). This indicates that whilst HOX genes present potential therapeutic targets, significant challenges remain. Nevertheless, a number of small molecular inhibitors of the interaction between HOX genes and their co-factor PBX have been developed, including HXR9 (Morgan *et al*, 2012). Identification of consistent changes in

specific HOX genes in particular cancers may present novel therapeutic targets or prognostic markers which can be exploited to improve clinical outcomes.

As the preliminary array data suggested increased expression of HOXD10 in SCC cells when compared to normal keratinocytes, this study aimed to validate this observation and understand the role high HOXD10 expression may play in HNSCC development.

Materials and methods

Cell Culture:

Head and neck squamous cell carcinoma (HNSCC) cell lines, oral pre-malignant (OPL), primary normal oral keratinocytes (NOK), and immortalized normal oral keratinocytes (iNOKs) (Table S3) were maintained in KGM (DMEM supplemented with 23% Ham's F-12, 10% FCS, L-glutamine (2mM), adenine (0.18mM), hydrocortisone (0.5µg/mL) and insulin (5µg/mL) (Sigma Aldrich, Cambridge, UK) at 37°C and 5% CO_2. Primary NOKs were isolated as previously described (Hearnden *et al*, 2009).

RNA extraction and qPCR:

Total RNA was extracted using the ISOLATE RNA mini kit (Bioline Reagents Ltd, London, UK) before quantification and purity assessment (A260/280 ≥1.9) using NanoDrop Spectrophotometer (Fisher Scientific, Loughborough, UK). cDNA was generated using the High Capacity cDNA Reverse Transcription kit (Life Technologies, Paisley, UK) with random primers or miR-specific stem-loop primers (Life Technologies, Paisley, UK). TaqMan probes and primers (Life Technologies, Paisley, UK) or primers for SYBR green chemistry (Sigma Aldrich, Cambridge, UK; table S3) were used to amplify target sequences by qPCR (7900HT thermocycler, Life Technologies, Paisley, UK). Data were analysed using RQ Manager 1.2.1 software (Life Technologies, Paisley, UK).

Antibodies:

Antibodies used were goat polyclonal anti-HOXD10 (Santa Cruz Biotechnology, Dallas, USA), rabbit polyclonal anti-HOXD10, rabbit polyclonal anti-AMOT-p80 (both Abcam, Cambridge, UK), and mouse monoclonal anti-β-actin (Sigma Aldrich, Cambridge, UK), anti-goat IgG horseradish peroxidase (HRP) (Amersham Ltd., Amersham, UK), anti-rabbit IgG HRP (New England Biolabs, Hitchin, UK), and anti-mouse IgG HRP (Cell Signalling, Hitchin, UK).

Western Blotting:

Cell pellets were lysed using RIPA buffer (Sigma Aldrich, Cambridge, UK) containing protease and phosphatase inhibitors (Roche, West Sussex, UK) and extracted proteins quantified using BCA method

(Smith *et al*, 1985). Protein extracts (100µg) were loaded onto 12% (v/v) SDS-PAGE, followed by wet transfer to nitrocellulose. Following incubation in blocking buffer (5% milk and 3% BSA in TBS containing 0.05% Tween-20) for 1 h membranes were incubated overnight at 4°C with anti-HOXD10 (1:250) or AMOT-p80 (1:250) antibodies. Membranes were incubated in anti-goat IgG HRP (1:50,000) or anti-rabbit IgG HRP (1:3000) antibodies for 1h at room temperature and developed with SuperSignal west pico chemiluminescent substrate (Fisher Scientific, Loughborough, UK).

Immunohistochemistry (IHC):

HOXD10 protein expression was assessed in a tissue microarray containing normal oral mucosa, OPL, primary HNSCC and metastases. AMOT-p80 expression was assessed in a smaller sub-panel of normal and HNSCC tissues. Microwave or pressure cooker antigen retrieval was used and samples were incubated with the primary antibody, rabbit anti-HOXD10 (1:50) or rabbit anti-AMOT-p80 (1:50), overnight at 4°C. Vectastain Elite ABC Rabbit IgG kit (Vector Ltd, Peterborough, UK) was used for the secondary antibody step followed by colour development using DAB. Specificity of the antibody was assessed by pre-adsorption with the immunogenic peptide (Abcam, Cambridge, UK). Staining was assessed using the Quickscore method(Detre *et al*, 1995).

HOXD10 and AMOT-p80 plasmid construction:

Primers amplifying the coding regions of HOXD10 and AMOT-p80 included a (CACC) sequence to aid insertion into pcDNA3.1-TOPO mammalian expressing vector (Life Technologies, Paisley, UK); HOXD10 forward : 5'-CACCATGTCCTTTCCCAACAGCT-3', reverse: 5'-CTAAGAAAACGTGAGGTTGGCGG-3', AMOT-p80 forward: 5'-CACCATGCCTCGGGCTCAGCCATCCTC-3', reverse: 5'-TTAGATGAGATATTCCACCATCTCTGCATCAGGCTCTTGTC-3'. Successful cloning of target sequences was confirmed by sequencing.

Plasmid, shRNA, and siRNA transfection

Cells were transfected in 6-well plates with pcDNA3.1-control, pcDNA3.1-HOXD10, pcDNA3.1-AMOT, control shRNA, or HOXD10 shRNA plasmids DNA (1µg/well) using FuGENE HD (Promega, Southampton, UK) while HOXD10 siRNA (OriGene, Rockville, USA) transfection was carried out at 50nM final concentration with Oligofectamine (Invitrogen, Loughborough, UK), as per the manufacturer's protocol. Following transfection, cells were incubated for 48-72h in their normal media before use in phenotypic or gene expression analyses. Stably transfected cells were selected using G418 (400µg/ml; Fisher, Loughborough, UK) in a 12-well plate for two weeks. Selected colonies were expanded and cells were grown in antibiotic containing media to maintain selection pressure. Transfection efficiency was confirmed by qPCR and western blotting.

Proliferation and apoptosis Assays:

Cells were seeded (4000 cells/well) in a 96-well plate in triplicate for each time point in DMEM supplemented with 10% (v/v) FCS. At each time point, wells were washed with PBS before adding 100µL serum-free DMEM medium and MTS reagent (Promega, Southampton, UK). Absorbance was read at 490nm using a microplate spectrophotometer (Tecan Ltd, Theale, UK).

Apoptotic cells were quantified using the TACS Annexin V-FITC Apoptosis Detection Kit (R&D systems, Abingdon, UK). Cells were cultured in tissue culture flasks in their respective medium until 80 % confluent, trysinised and 5x105 cells transferred to a microtube. Cells were washed in ice-cold PBS containing 0.1% BSA, resuspended in binding buffer and incubated with Annexin V-FITC and propidium iodide according to the manufacturer's instructions. Cells were analysed using a LSR II flow cytometer (BD Biosciences, San Jose, CA, USA).

Adhesion Assay:

A 96-well plate was coated with 0.1% (w/v) fibronectin (Sigma Aldrich, Cambridge, UK) diluted in PBS and kept overnight at 4ºC. On the following day, wells were washed with PBS and incubated with DMEM containing 1% (w/v) BSA for 1h. Cells (30,000 cells/well) were seeded in serum-free DMEM medium and incubated for 1h at 37ºC. Non-adherent cells were removed by washing with PBS before adding 100µL serum-free DMEM medium and MTS reagent, and absorbance measured as described.

Transwell Migration and Invasion Assays:

To assess migration, 60,000 cells, serum starved for 24 hours, resuspended in DMEM with 0.1% (w/v) BSA and placed in the top chamber of a 24-well Transwell insert (8µM: BD Biosciences, Oxford, UK). DMEM was added to the bottom well with 2% (v/v) FCS and incubated overnight at 37ºC for 16h. Migrated cells were stained with crystal violet and counted. To assess cell invasion, a similar protocol was followed with prior coating of the membrane with 100µL of growth factor-reduced Matrigel (BD Biosciences, Oxford, UK) diluted in PBS (1:45). Mitomycin C was used at a concentration of 1 ug/mL at both the cell suspension and at the chemoattractant-containing medium in the lower chamber to stop any cell division during the assay.

Agilent microarray:

Total RNA was extracted from triplicate cultures of B22 and D19 cells stably transfected with either pcDNA3.1-HOXD10 or pcDNA3.1-control, and T5 and D35 cells transfected with either HOXD10 siRNA or scrambled siRNA control. RNA quality was assessed using an Agilent Bioanalyser (28s:18s ≥ 2:1 and RIN=10). Sample labelling was carried out as per the manufacturer's protocol before hybridization onto SurePrintG3 Human Oligo arrays (Agilent). After 17 hours, hybridized slides scanned at 3µm

resolution using Agilent C Microarray Scanner. The data was loaded into Genespring (version 12.5), normalised by the Quartile method and analysed using One-way ANOVA (Welch) with Benjamini-Hochberg correction to identify significantly differentially expressed genes with a fold change >2.

The list of significantly differentially expressed genes was filtered criteria to enrich for putative targets of HOXD10. Firstly, genes which showed reciprocal changes in expression with HOXD10 overexpression and knockdown were selected. Next, the promoter regions of the remaining genes were detected and screened for HOXD10 binding sites using PROMO online algorithm (Messeguer *et al*, 2002) (http://alggen.lsi.upc.es/cgi-bin/promo_v3/promo/promoinit.cgi?dirDB=TF_8.3). Lastly, the overall pattern of expression was assessed and compared with HOXD10 expression in a cell panel.

Cloning of wild-type and mutated AMOT-p80 and miR-146a promoters:

The putative promoter regions of AMOT-p80 and miR-146a were identified using in-silico analysis using http://rulai.cshl.edu/cgi-bin/CSHLmpd2/promExtract.pl?species=Human (Zhang, 2003), http://biowulf.bu.edu/zlab/PromoSer/ (Halees *et al*, 2003), and http://www.genomatix.de/solutions/genomatix-software-suite.html (Cartharius *et al*, 2005). To clone the promoter sequences into pGL3-basic luciferase reporter vector, sequences of *XhoI* and *HindIII* restriction sites were added to forward and reverse primers, respectively (restriction sites underlined): AMOT-p80 promoter forward: 5'- TGCTAACTCTCGAGAGTCAACTTCATATCCACCCCCAAAA-3', reverse: 5'-TACGCCAAGCTTACGACCAAGTTCATGCCACCAT-3', miR-146a promoter forward: 5'-AAAATTCTCGAGTTGAAAAGCCAACAGGCTCATTGG-3', reverse: 5'-CAAATTTAAGCTTCCACTCCAATCGGCCCTGCT-3'.

HOXD10 binding sites in AMOT-p80 and miR-146a were predicted using PROMO algorithm: http://alggen.lsi.upc.es/cgi-bin/promo_v3/promo/promoinit.cgi?dirDB=TF_8.3 (Messeguer *et al*, 2002). Using mutagenic PCR method, random nucleotides in the binding site were substituted with different nucleotides to impair HOXD10 binding. pGL3-AMOT and pGL3-miR-146a wild-type (WT) sequence was used as the templates in this PCR. The primers used for mutation of the HOXD10 binding site in addition to the cloning forward and reverse primers were as follows, (mutated bases in bold): AMOT-p80 mutagenic forward: 5'-CACAATAGCCTCTTGTTTAGT**CC**TATTAATTTTGAGGGCGGGTGG-3', reverse: 5'-CCACCCGCCCTCAAAATTAATA**GG**ACTAAACAAGAGGCTATTGTG-3', miR-146a mutagenic forward: 5'-AGGGTGTGGAAATGGAATA**TTT**GCATATGCAAATAGGCCTT-3', reverse: 5'-AAGGCCTATTTGCATATGC**AAA**TATTCCATTTCCACACCCT-3'. Successful cloning was confirmed by sequencing.

Dual Luciferase Reporter (DLR) Assay

Cloned pGL3-AMOT and pGL3-miR-146a wild-type (WT) and mutated promoters were transfected using FuGENE HD (Promega, Southampton, UK) into cells stably expressing pcDNA3.1-HOXD10 DNA or pcDNA3.1-control. To confirm transfection efficacy and to normalise the firefly luciferase expression, constructs were co-transfected with a pRL-TK *Renilla* internal control vector in a ratio of 1:10. Forty-eight hours post-transfection, cells were lysed and expression levels of firefly and *Renilla* luciferase were determined using the DLR assay kit (Promega, Southampton, UK) and a GloMax luminometer (Promega, Southampton, UK) as per the manufacturer's instructions.

Statistical Analysis:

Non-parametric Kruskal-Wallis test was performed on the IHC scoring for HOXD10 in SPSS (IBM, New York, NY, USA). One-way ANOVA (Welch) was used to identify differentially expressed genes in the microarray data using Benjamini-Hochberg correction. Otherwise, student's T-test was used, unless otherwise stated. Differences were considered statistically significant if $p \leq 0.05$.

Ethics

Ethics approval for the use of tissues was obtained from The West Glasgow LREC (08/S0709/70). Ethical approval for the NOK primary cultures used was obtained from Sheffield LREC (09/H1308/66).

Results

HOXD10 expression in HNSCC

Validation of the initial microarray data by qPCR and WB demonstrated high HOXD10 expression in cells from primary HNSCCs compared to NOKs, but this elevated expression was not observed in cell cultures from lymph node metastases, B22 and TR146 (Figure 1A and Figure S1). Expression in the cultures from OPLs was variable, although some, e.g. D35, did express HOXD10 at high levels. No clear relationship between the static level of expression of HOXD10 and that of known interacting molecules such as miR-7, miR-10b, and IGFBP3, was seen (Supplementary figure S2).

In tissues, HOXD10 was expressed in the nucleus and the cytoplasm. This is similar to reports of a number of other HOX genes(Abe *et al*, 2006) and may represent shuttling between the nucleus and the cytoplasm(Ziegler & Ghosh, 2005). Analysis of HOXD10 expression in a Tissue Microarray (TMA) from different phases of HNSCC development demonstrated increased expression of HOXD10 in primary tumours and loss of expression in metastases, similar to expression changes observed *in vitro* (Figure 1B and 1C). The OPL tissues (with a range of grades of dysplasia), demonstrate an intermediate pattern of HOXD10 expression, which is variable. Further analysis in TMA constructed from a cohort of

27 matched HNSCC primary tumours and metastases confirmed the pattern with expression lower in the metastases of 23/27 patients (85%; Figure 1D).

Effects of manipulation of HOXD10 expression

Firstly, we assessed the phenotypic consequences of transfecting HOXD10 into low-HOXD10 expressing OPL and metastatic HNSCC cells. Stable over-expression of HOXD10 was achieved in two cell lines, D19 (OPL) and B22 (metastasis), and confirmed by both qPCR and Western blot (Figure 2A). Increasing the expression of HOXD10 resulted in an increase in migration, adhesion to fibronectin and cell proliferation (Figure 2B, 2C and 2D), but a decrease in cell invasion (Figure 2E). The proportion of apoptotic cells in D19 was unchanged, but a small increase was seen in B22 (Figure S3A and S3B). Conversely, knockdown of HOXD10 was achieved by siRNA and confirmed by qPCR in high-HOXD10 expressing D35 (OPL) and T5 (HNSCC) cells (Figure 3A). This resulted in a decrease in migration, adhesion to fibronectin and proliferation, and an increase in invasion (Figure 3B, 3C, 3D and 3E), eliciting opposite effects to those seen on HOXD10 over-expression. There was no change in the proportion of apoptotic cells (Figure S3C and S3D).

Microarray analysis of transfected cells

To identify the pathways and individual genes through which HOXD10 exerts these effects, we conducted expression microarray analysis of cells with stable HOXD10 over-expression (D19+ and B22+) or knockdown (D35- and T5-). After normalisation, data analysis yielded 9167 genes whose expression was significantly reciprocally altered in HOXD10 over-expressing and siRNA transfected cells. The list was refined to 414 genes, using an overall fold change of >2. Gene Ontology (GO) mapping of the differentially expressed genes identified a number of significantly enriched GO categories (Table S1). These map to the effects seen in the cells on the manipulation of HOXD10.

Validation of putative HOXD10 target genes

After further filtering by *in-silico* analysis, a final list of 48 differentially expressed genes were identified as putative targets of HOXD10 (Figure 4A, Table (S2). Using qPCR analysis, the expression level of the selected 48 HOXD10 putative targets were assessed in the manipulated cells and also in the whole panel of cell lines (data not shown). 39 of these genes showed a negative or positive correlation between their expression and HOXD10 expression in both HOXD10-manipulated cells and a panel of cell lines. The top 8 differentially expressed genes are shown in Figure 4B, selected on the basis of close relation to HOXD10 expression and *in silico* analysis for putative HOXD10 binding sites in the promoter; the two candidates which most closely matched HOXD10 expression were angiomotin (transcript variant 2, AMOT-p80) and miR-146a.

Immunoblotting showed that AMOT-p80 protein expression increased after HOXD10 transfection in low expressing OPM and HNSCC cells (Figure 5A) but was reduced in high expressing (D35 and T5) cells transfected with HOXD10 siRNA (Figure 5B), in keeping with the microRNA data. AMOT-p80 expression was also assessed in a wider panel of NOKs, OPL and HNSCC cells, showing a pattern of expression that is similar to that of HOXD10 (Supplementary Figure S5C and S5D). miR-146a expression decreased after HOXD10 transfection in low expressing OPL and HNSCC cells (Figure 5C) and was induced after HOXD10 siRNA transfection into high expressing cells (Figure 5D). miR-146a expression was also assessed in the same panel of NOKs, OPL and HNSCC cells, showing high expression in normal cells, and low expression in HNSCC cells, which suggests a negative correlation with HOXD10 expression level (Supplementary Figure S5A and S5B).

Investigation of AMOT-p80 and miR146a promoters as direct targets of HOXD10

HOXD10 over-expression increased luciferase activity from a wild-type AMOT-p80 promoter reporter construct (Figure 5E). This was not observed after mutation of the putative HOXD10-binding sites in the promoter (Fig 5E), indicating a direct effect of HOXD10 on AMOT-p80 expression at a transcriptional level. The effect was further increased by mutating more than one HOXD10-binding site. HOXD10 over-expression suppressed luciferase activity from a wild-type miR-146 promoter reporter construct (Figure 5F). This was not observed after mutation of the putative HOXD10-binding site (Figure 5F), indicating that HOXD10 directly suppresses miR-146a expression by interacting with its promoter.

The function of AMOT-p80 in HNSCC cells

Transient transfection of AMOT-p80 into HNSCC cells which express low levels of HOXD10 and AMOT (B22 and D19, expression confirmed by qPCR and WB in Figure 6A) resulted in similar phenotypic changes to transfection with HOXD10; there was an increase in proliferation and migration of cells (Figure 6B and 6C). There was no effect on adhesion to fibronectin (Figure 6D).

Transfection of AMOT-p80 into cells stably depleted of HOXD10 (Figure 7A) rescued the phenotype, with partial reversal of the reduction in proliferation (Figure 7B) and reversion of migration to a level higher than original control levels (Figure 7C). Assessment of expression of AMOT-p80 in a panel of normal oral mucosa and HNSCC tissues showed that the expression of AMOT-p80 was much higher in the HNSCC samples, where there was both cytoplasmic and nuclear expression of AMOT-p80 (in keeping with a recent report in hepatocellular tumorigenesis (Yi *et al*, 2013)) with focal light cytoplasmic expression in normal oral mucosa (Figure 7D).

Discussion

Various HOX genes have been described to play a role in the development of a wide range of cancers. The role of HOXA cluster genes in haemato-lymphoid cancers has been extensively investigated, resulting in the identification of a number of fusion proteins (for example NUP98:HOXC11) which results in aberrant HOX trans-regulatory activity. In primary breast cancers, HOXA5, HOXA9 and HOXB13 are down-regulated whereas HOXB9 and HOXD10 are up-regulated (Chen *et al*, 2004; Gilbert *et al*, 2010; Ma *et al*, 2007). Changes in the expression of other HOX genes have been reported in lung and gastric cancers (Abe *et al*, 2006). In HNSCC, several HOX genes, including HOXA5, HOXD10 and HOXD11 show higher levels of expression in oral cancer tissues compared to normal tissues (Rodini *et al*, 2012). Although high expression levels of HOXD10 have previously been observed in invasive oral cancers, this is the first study to explore the functional roles of HOXD10 in HNSCC development. We also demonstrate that HOXD10 expression is reduced in HNSCC metastases relative to their paired primary tumours.

We show that HOXD10 promotes the proliferation, migration and adhesion to fibronectin of primary HNSCCs cells, with no consistent effect on apoptosis, by demonstrating reciprocal phenotypic changes on over-expression of knockdown of HOXD10. These effects may promote the development of the primary tumour as it becomes established at the primary site. This is supported by the observation that some OPL cells also express high levels of HOXD10. Thus, it is likely that increasing HOXD10 expression during HNSCC development supports the emergence of cells which populate the primary tumour. Interestingly, the observations that HOXD10 supresses invasion into matrigel, that expression of HOXD10 is low in cells derived from metastases, and that the tumour loses expression of HOXD10 in its metastases suggest a change in the role HOXD10 is playing as cancer develops and spreads to sites distant to the primary tumour. Inhibition of invasion by HOXD10 would indicate anti-metastatic properties, which have been demonstrated in other cancer types (Ma *et al*, 2010). The overall pattern of high primary tumour HOXD10 expression, with loss of expression in metastases which we have observed, has been reported in other cancers, such as bladder cancer (Baffa *et al*, 2009). Furthermore, in breast cancer, tumorigenic but non-metastatic breast cancer cells lines express little or no miR-10b, which down-regulates HOXD10 expression, in keeping with high HOXD10 expression (Ma *et al*, 2007). However, this does not seem to be a consistent pattern across all cancers, as in primary gastric cancers HOXD10 is down-regulated by promoter methylation, which profoundly inhibits proliferation and migration (Wang *et al*, 2012). This highlights the context and cell-specific roles of these transcription factors, particularly as their expression may be regulated by a number of different mechanisms.

In breast and gastric cancer cells, high expression of miR-10b activates signalling via the RhoC-AKT signalling pathway which promotes migration and invasion (Liu *et al*, 2012; Ma *et al*, 2007). Our phenotypic assessment of the effects of HOXD10 in HNSCC cells indicates that low expression of

HOXD10 is associated with increased invasive potential and the expression microarray analysis of these cells indicates that low HOXD10 expression increases the expression of a number of known modulators of epithelial-mesenchymal transition (EMT; Figure S4 and Table S2). Indeed, recent investigations in stem cell programming and cancer have demonstrated that miR-10b (and other microRNAs) modulate EMT(Han *et al*, 2014), which is also known to be an important part of the pro-metastatic phenotype cancer cells derive as they develop. The direct link to HOXD10, however, has not been made in this context.

The mechanism of down-regulation of HOXD10 in HNSCC as it metastasises is not clear. In contrast to that seen in breast and ovarian cancer, there is no direct relationship between the expression of HOXD10 and miR-10b in HNSCC, (Figure S2), in keeping with other work in the field(Severino *et al*, 2013). Our unpublished observations also suggest that down-regulation is not due to promoter methylation in these HNSCC cells (data not shown). Thus, there is scope for further investigation of other potential mechanisms of modulation of HOXD10 in keratinocytes, both in terms of the initiating promotion of expression and its subsequent loss in lymph node metastases. Other suggestions include the possible role of long non-coding RNAs such as HOTAIR, however these effects also appear to be tumour specific (Nakayama *et al*, 2013).

The differential pattern of expression observed here poses interesting questions regarding the possible uses of HOXD10 both as a biomarker and potential therapeutic target. Of the tumours which metastasized, all demonstrated the pattern of high expression in the primary tumour, low expression in metastases. No significant association of loss of HOXD10 expression in the primary tumour with the presence of metastasis was identified, thus it is unlikely to be useful as a prognostic biomarker. Similarly, it is not likely to be a potential therapeutic target in itself, as both high and low expression, in the correct context, can support development and progression of the tumour. Nevertheless, its possible utility as a marker of progression of OPLs to HNSCC warrants further investigation, given the high expression in some OPL cells and tissues which may be related to risk of progression to invasive disease. Also, as HOXD10 is acting as a transcription factor, identification of the targets of HOXD10 at the particular stage of disease development indicated may identify useful biomarkers or novel therapeutic targets.

We used expression microarray analysis to identify possible targets of HOXD10. Although this approach has acknowledged limitations, our algorithm for target identification was successful in the identification of a number of novel direct HOXD10 targets, including angiomotin (AMOT-p80) and miR-146a.

miR-146a is well established as an inhibitor of cell proliferation and as a suppressor of metastasis (Chen *et al*, 2013; Hurst *et al*, 2009; Yao *et al*, 2013), and thus the finding that HOXD10 decreases miR-

146a expression is in keeping with the observed phenotype. We therefore conducted detailed investigation on the role of the novel identified target, AMOT-p80, understanding of which in the context of cancer biology is limited.

The angiomotin family of proteins, of which there are 3 members (AMOT, AMOTL1 and AMOTL2), belong to the motin family of angiostatin-binding proteins and are involved in regulation of cell growth and motility. They have been localised in close association with tight junctions, whose enhanced turnover has been associated with promotion of tumour development in HNSCC (Vilen *et al*, 2012). Two isoforms of AMOT have been identified (p80 and p130), with the increased expression of AMOT-p80 associated with increased migration of endothelial cells (Ernkvist *et al*, 2008). The activity of AMOT-p80 is inhibited by the 4.1 protein superfamily member, Merlin, in a complex at tight junctions which includes YAP, LATS and other AMOT family members (Paramasivam *et al*, 2011). Recent investigations have demonstrated that AMOT-p80 opposes the activation of signalling pathways by other AMOT family members, including activation of tumour suppressors YAP and LATS2 (Zhao *et al*, 2011). Others have shown that AMOT-p80 promotes tumour growth in a number of different contexts: signalling via RAS-MAPK to promote both proliferation of embyronal kidney cell lines and enhanced development of xenograft tumours in mice using NF2 null Schwann cells (Yi *et al*, 2011); signalling via ERK1/2 in breast cancer cells, resulting in increased proliferation and dysregulated cell polarity which resulted in a more neoplastic growth pattern (Ranahan *et al*, 2011). Our data in HNSCC supports the role of AMOT-p80 in the promotion of tumour growth, although it is not clear if HOXD10 plays a role in control of AMOT-p80 expression in these other tumour types. Nevertheless, AMOT-p80 is a potential target for novel therapeutics which may be useful in a number of cancers. Both AMOT-p80 and miR-146a, identified here as novel HOXD10 targets, may represent therapeutic targets at particular tumour promoting stages.

Acknowledgements

The authors would like to thank Dr Adam Jones and Mrs Ibtisam Zargoun for the TMAs in this project and Dr Helen Colley for her assistance with the apoptosis assays. FH is supported by the Government of the Kingdom of Saudi Arabia.

Conflict of Interest statement:

All of the authors confirm that they have no conflict of interest to declare.

References

Abe M, Hamada J, Takahashi O, Takahashi Y, Tada M, Miyamoto M, Morikawa T, Kondo S, Moriuchi T (2006) Disordered expression of HOX genes in human non-small cell lung cancer. *Oncol Rep* **15**(4)**:** 797-802

Agrawal N, Frederick MJ, Pickering CR, Bettegowda C, Chang K, Li RJ, Fakhry C, Xie TX, Zhang J, Wang J, Zhang N, El-Naggar AK, Jasser SA, Weinstein JN, Trevino L, Drummond JA, Muzny DM, Wu Y, Wood LD, Hruban RH, Westra WH, Koch WM, Califano JA, Gibbs RA, Sidransky D, Vogelstein B, Velculescu VE, Papadopoulos N, Wheeler DA, Kinzler KW, Myers JN (2011) Exome sequencing of head and neck squamous cell carcinoma reveals inactivating mutations in NOTCH1. *Science* **333**(6046)**:** 1154-7

Baffa R, Fassan M, Volinia S, O'Hara B, Liu CG, Palazzo JP, Gardiman M, Rugge M, Gomella LG, Croce CM, Rosenberg A (2009) MicroRNA expression profiling of human metastatic cancers identifies cancer gene targets. *J Pathol* **219**(2)**:** 214-21

Cartharius K, Frech K, Grote K, Klocke B, Haltmeier M, Klingenhoff A, Frisch M, Bayerlein M, Werner T (2005) MatInspector and beyond: promoter analysis based on transcription factor binding sites. *Bioinformatics* **21**(13)**:** 2933-42

Chen G, Umelo IA, Lv S, Teugels E, Fostier K, Kronenberger P, Dewaele A, Sadones J, Geers C, De Greve J (2013) miR-146a inhibits cell growth, cell migration and induces apoptosis in non-small cell lung cancer cells. *PLoS One* **8**(3)**:** e60317

Chen H, Chung S, Sukumar S (2004) HOXA5-induced apoptosis in breast cancer cells is mediated by caspases 2 and 8. *Mol Cell Biol* **24**(2)**:** 924-35

Detre S, Saclani Jotti G, Dowsett M (1995) A "quickscore" method for immunohistochemical semiquantitation: validation for oestrogen receptor in breast carcinomas. *J Clin Pathol* **48**(9)**:** 876-8

Dickson MA, Hahn WC, Ino Y, Ronfard V, Wu JY, Weinberg RA, Louis DN, Li FP, Rheinwald JG (2000) Human keratinocytes that express hTERT and also bypass a p16(INK4a)-enforced mechanism that limits life span become immortal yet retain normal growth and differentiation characteristics. *Mol Cell Biol* **20**(4)**:** 1436-47

Edington KG, Loughran OP, Berry IJ, Parkinson EK (1995) Cellular immortality: a late event in the progression of human squamous cell carcinoma of the head and neck associated with p53 alteration and a high frequency of allele loss. *Mol Carcinog* **13**(4)**:** 254-65

Eklund EA (2007) The role of HOX genes in malignant myeloid disease. *Current opinion in hematology* **14**(2)**:** 85-9

Ernkvist M, Birot O, Sinha I, Veitonmaki N, Nystrom S, Aase K, Holmgren L (2008) Differential roles of p80- and p130-angiomotin in the switch between migration and stabilization of endothelial cells. *Biochim Biophys Acta* **1783**(3)**:** 429-37

Gilbert PM, Mouw JK, Unger MA, Lakins JN, Gbegnon MK, Clemmer VB, Benezra M, Licht JD, Boudreau NJ, Tsai KK, Welm AL, Feldman MD, Weber BL, Weaver VM (2010) HOXA9 regulates BRCA1 expression to modulate human breast tumor phenotype. *J Clin Invest* **120**(5)**:** 1535-50

Halees AS, Leyfer D, Weng Z (2003) PromoSer: A large-scale mammalian promoter and transcription start site identification service. *Nucleic Acids Res* **31**(13)**:** 3554-9

Han X, Yan S, Weijie Z, Feng W, Liuxing W, Mengquan L, Qingxia F (2014) Critical role of miR-10b in transforming growth factor-beta1-induced epithelial-mesenchymal transition in breast cancer. *Cancer Gene Ther*

Hearnden V, Lomas H, Macneil S, Thornhill M, Murdoch C, Lewis A, Madsen J, Blanazs A, Armes S, Battaglia G (2009) Diffusion studies of nanometer polymersomes across tissue engineered human oral mucosa. *Pharm Res* **26**(7)**:** 1718-28

Hunter KD, Thurlow JK, Fleming J, Drake PJ, Vass JK, Kalna G, Higham DJ, Herzyk P, Macdonald DG, Parkinson EK, Harrison PR (2006) Divergent routes to oral cancer. *Cancer Res* **66**(15)**:** 7405-13

Hurst DR, Edmonds MD, Scott GK, Benz CC, Vaidya KS, Welch DR (2009) Breast Cancer Metastasis Suppressor 1 Up-regulates miR-146, Which Suppresses Breast Cancer Metastasis. *Cancer Research* **69**(4)**:** 1279-1283

Leemans CR, Braakhuis BJ, Brakenhoff RH (2011) The molecular biology of head and neck cancer. *Nat Rev Cancer* **11**(1)**:** 9-22

Liu Z, Zhu J, Cao H, Ren H, Fang X (2012) miR-10b promotes cell invasion through RhoC-AKT signaling pathway by targeting HOXD10 in gastric cancer. *Int J Oncol* **40**(5)**:** 1553-60

Ma L, Reinhardt F, Pan E, Soutschek J, Bhat B, Marcusson EG, Teruya-Feldstein J, Bell GW, Weinberg RA (2010) Therapeutic silencing of miR-10b inhibits metastasis in a mouse mammary tumor model. *Nat Biotechnol* **28**(4)**:** 341-7

Ma L, Teruya-Feldstein J, Weinberg R (2007) Tumour invasion and metastasis initiated by microRNA-10b in breast cancer. *Nature* **449**(7163)**:** 682-8

McGregor F, Muntoni A, Fleming J, Brown J, Felix DH, MacDonald DG, Parkinson EK, Harrison PR (2002) Molecular changes associated with oral dysplasia progression and acquisition of immortality: potential for its reversal by 5-azacytidine. *Cancer Res* **62**(16)**:** 4757-66

Messeguer X, Escudero R, Farre D, Nunez O, Martinez J, Alba MM (2002) PROMO: detection of known transcription regulatory elements using species-tailored searches. *Bioinformatics* **18**(2)**:** 333-4

Morgan R, Boxall A, Harrington KJ, Simpson GR, Gillett C, Michael A, Pandha HS (2012) Targeting the HOX/PBX dimer in breast cancer. *Breast Cancer Res Treat* **136**(2)**:** 389-98

Nakayama I, Shibazaki M, Yashima-Abo A, Miura F, Sugiyama T, Masuda T, Maesawa C (2013) Loss of HOXD10 expression induced by upregulation of miR-10b accelerates the migration and invasion activities of ovarian cancer cells. *Int J Oncol* **43**(1)**:** 63-71

Paramasivam M, Sarkeshik A, Yates JR, Fernandes MJG, McCollum D (2011) Angiomotin family proteins are novel activators of the LATS2 kinase tumor suppressor. *Molecular Biology of the Cell* **22**(19)**:** 3725-3733

Picchi J, Trombi L, Spugnesi L, Barachini S, Maroni G, Brodano GB, Boriani S, Valtieri M, Petrini M, Magli MC (2013) HOX and TALE signatures specify human stromal stem cell populations from different sources. *J Cell Physiol* **228**(4)**:** 879-89

Pickering CR, Zhang J, Yoo SY, Bengtsson L, Moorthy S, Neskey DM, Zhao M, Ortega Alves MV, Chang K, Drummond J, Cortez E, Xie TX, Zhang D, Chung W, Issa JP, Zweidler-McKay PA, Wu X, El-Naggar AK, Weinstein JN, Wang J, Muzny DM, Gibbs RA, Wheeler DA, Myers JN, Frederick MJ (2013) Integrative genomic characterization of oral squamous cell carcinoma identifies frequent somatic drivers. *Cancer discovery* **3**(7)**:** 770-81

Prime SS, Nixon SV, Crane IJ, Stone A, Matthews JB, Maitland NJ, Remnant L, Powell SK, Game SM, Scully C (1990) The behaviour of human oral squamous cell carcinoma in cell culture. *J Pathol* **160**(3)**:** 259-69

Ranahan WP, Han Z, Smith-Kinnaman W, Nabinger SC, Heller B, Herbert BS, Chan R, Wells CD (2011) The Adaptor Protein AMOT Promotes the Proliferation of Mammary Epithelial Cells via the Prolonged Activation of the Extracellular Signal-Regulated Kinases. *Cancer Research* **71**(6)**:** 2203-2211

Rice KL, Licht JD (2007) HOX deregulation in acute myeloid leukemia. *J Clin Invest* **117**(4)**:** 865-8

Rinn JL, Kertesz M, Wang JK, Squazzo SL, Xu X, Brugmann SA, Goodnough LH, Helms JA, Farnham PJ, Segal E, Chang HY (2007) Functional demarcation of active and silent chromatin domains in human HOX loci by Noncoding RNAs. *Cell* **129**(7)**:** 1311-1323

Rodini CO, Xavier FC, Paiva KB, De Souza Setubal Destro MF, Moyses RA, Michaluarte P, Carvalho MB, Fukuyama EE, Head, Neck Genome Project G, Tajara EH, Okamoto OK, Nunes FD (2012) Homeobox gene expression profile indicates HOXA5 as a candidate prognostic marker in oral squamous cell carcinoma. *Int J Oncol* **40**(4)**:** 1180-8

Rupniak HT, Rowlatt C, Lane EB, Steele JG, Trejdosiewicz LK, Laskiewicz B, Povey S, Hill BT (1985) Characteristics of four new human cell lines derived from squamous cell carcinomas of the head and neck. *J Natl Cancer Inst* **75**(4)**:** 621-35

Severino P, Bruggemann H, Andreghetto FM, Camps C, Klingbeil Mde F, de Pereira WO, Soares RM, Moyses R, Wunsch-Filho V, Mathor MB, Nunes FD, Ragoussis J, Tajara EH (2013) MicroRNA expression profile in head and neck cancer: HOX-cluster embedded microRNA-196a and microRNA-10b dysregulation implicated in cell proliferation. *BMC Cancer* **13:** 533

Smith PK, Krohn RI, Hermanson GT, Mallia AK, Gartner FH, Provenzano MD, Fujimoto EK, Goeke NM, Olson BJ, Klenk DC (1985) Measurement of protein using bicinchoninic acid. *Anal Biochem* **150**(1)**:** 76-85

Vilen ST, Suojanen J, Salas F, Risteli J, Ylipalosaari M, Itkonen O, Koistinen H, Baumann M, Stenman UH, Sorsa T, Salo T, Nyberg P (2012) Trypsin-2 enhances carcinoma invasion by processing tight junctions and activating ProMT1-MMP. *Cancer Invest* **30**(8)**:** 583-92

Wang LJ, Chen SJ, Xue M, Zhong J, Wang X, Gan LH, Lam EKY, Liu X, Zhang JB, Zhou TH, Yu J, Jin HC, Si JM (2012) Homeobox D10 Gene, a Candidate Tumor Suppressor, Is Downregulated through Promoter Hypermethylation and Associated with Gastric Carcinogenesis. *Molecular Medicine* **18**(3)**:** 389-400

Wardwell-Ozgo J, Dogruluk T, Gifford A, Zhang Y, Heffernan TP, van Doorn R, Creighton CJ, Chin L, Scott KL (2013) HOXA1 drives melanoma tumor growth and metastasis and elicits an invasion gene expression signature that prognosticates clinical outcome. *Oncogene*

Wu X, Chen H, Parker B, Rubin E, Zhu T, Lee JS, Argani P, Sukumar S (2006) HOXB7, a homeodomain protein, is overexpressed in breast cancer and confers epithelial-mesenchymal transition. *Cancer Res* **66**(19)**:** 9527-34

Yao Q, Cao Z, Tu C, Zhao Y, Liu H, Zhang S (2013) MicroRNA-146a acts as a metastasis suppressor in gastric cancer by targeting WASF2. *Cancer Lett* **335**(1)**:** 219-24

Yi CL, Shen ZW, Stemmer-Rachamimov A, Dawany N, Troutman S, Showe LC, Liu Q, Shimono A, Sudol M, Holmgren L, Stanger BZ, Kissil JL (2013) The p130 Isoform of Angiomotin Is Required for Yap-Mediated Hepatic Epithelial Cell Proliferation and Tumorigenesis. *Science Signaling* **6**(291)

Yi CL, Troutman S, Fera D, Stemmer-Rachamimov A, Avila JL, Christian N, Persson NL, Shimono A, Speicher DW, Marmorstein R, Holmgren L, Kissil JL (2011) A Tight Junction-Associated Merlin-Angiomotin Complex Mediates Merlin's Regulation of Mitogenic Signaling and Tumor Suppressive Functions. *Cancer Cell* **19**(4)**:** 527-540

Zhang MQ (2003) Prediction, annotation, and analysis of human promoters. *Cold Spring Harbor symposia on quantitative biology* **68:** 217-25

Zhao B, Li L, Lu Q, Wang LH, Liu CY, Lei QY, Guan KL (2011) Angiomotin is a novel Hippo pathway component that inhibits YAP oncoprotein. *Gene Dev* **25**(1)**:** 51-63

Ziegler EC, Ghosh S (2005) Regulating inducible transcription through controlled localization. *Sci STKE* **2005**(284)**:** re6

Table S1

Term	Count	%	P Value	Genes	Fold Enrich-ment
GO:0001944~vasculature development	18	4.42	6.58E-05	FGF6, RECK, CAV1, PDPN, PRRX1, ARHGAP24, MMP14, EDNRA, VEGFC, SMO, NOTCH1, LAMA4, APOE, ZC3H12A, AMOT, MKL2, EGF, ANGPTL4	3.12
GO:0030856~regulation of epithelial cell differentiation	6	1.47	4.56E-04	CAV1, NOTCH1, CYP27B1, KRT36, CD24, AQP3	9.03
GO:0048870~cell motility	16	3.93	0.004711	CTHRC1, IL6, PF4, CUZD1, MMP14, DNAH5, SMO, VEGFC, DNER, CATSPER1, AMOT, POU4F1, LHX6, CD24, SCNN1G, AKAP4	2.27
GO:0048589~developmental growth	8	1.97	0.003721	DMBX1, SMO, NOTCH1, ALMS1, IGFBP1, TIMP3, PLAUR, HOXD11	4.01
GO:0042327~positive regulation of phosphorylation	10	2.46	3.70E-04	EDNRA, CSF2, VEGFC, CAV1, IL6, HCLS1, RICTOR, CD24, EGF, IL11	4.50
GO:0043565~sequence-specific DNA binding	23	5.65	0.01489	DMBX1, NANOG, FOXA2, HMBOX1, PRRX1, NR3C2, FOXN2, RORC, HMGA2, VSX1, HOXD10, HOXD11, FOXQ1, NOTCH1, FOXF2, LHX3, PBX1, POU4F1, LHX6, NFE2L3, FOXD1, FOSL1, ETV4	1.72
GO:0050708~regulation of protein secretion	6	1.474201	0.01027	VEGFC, PCSK1, IL6, CADM1, EGF, NLRP3	4.51

Table S2

Probe ID	Accession number	**Gene symbol**	*p* - value (ANOVA)	Effect of HOXD10 over-expression	Effect of HOXD10 silencing	Fold change
A_23_P207213	NM_000691	ALDH3A1	6.2E-04	+	-	4.1
A_23_P212508	NM_001063	TF	6.7E-04	+	-	3.7
A_33_P3322085	NM_001102651	ZNF554	1.4E-03	+	-	5.8
A_33_P3308744	NM_001105206	LAMA4	1.0E-02	+	-	3.1
A_33_P3235078	NM_001134855	TRIM17	4.2E-02	+	-	5.4
A_24_P388786	NM_001369	DNAH5	3.0E-05	+	-	3.3
A_23_P106024	NM_002226	JAG2	6.4E-04	+	-	2.8
A_24_P102053	NM_002538	OCLN	3.8E-02	+	-	3.9
A_23_P85693	NM_004120	GBP2	4.3E-08	+	-	2.9
A_33_P3336686	NM_004669	CLIC3	6.6E-10	+	-	3
A_23_P112482	NM_004925	AQP3	1.8E-03	+	-	3
A_23_P319859	NM_005244	EYA2	1.6E-04	+	-	2.7
A_33_P3369844	NM_013230	CD24	5.5E-04	+	-	3
A_23_P18447	NM_013261	PPARGC1A	5.2E-03	+	-	3.5
A_23_P204640	NM_024865	NANOG	4.2E-03	+	-	2.9
A_32_P164246	NM_033260	FOXQ1	1.8E-06	+	-	3.2
A_24_P344961	NM_133265	**AMOT**	9.0E-07	+	-	3.9
A_24_P383609	NM_199461	NANOS1	1.7E-03	+	-	3
A_33_P3318357	NM_138775	ALKBH8	1.3E-04	+	-	2.7
A_33_P3314902	NM_016252	BIRC6	1.1E-02	+	-	2.2
A_24_P365515	NM_021784	FOXA2	1.9E-02	+	-	2.8
A_23_P134454	NM_001753	CAV1	1.4E-02	+	-	2.3
A_33_P3277198	NM_004854	CHST10	7.0E-06	+	-	2.5
A_33_P3370424	NM_017617	NOTCH1	1.9E-03	+	-	2.1
A_33_P3627001	NM_144962	PEBP4	1.3E-03	+	-	2.3
A_23_P137035	NM_003662	PIR	1.5E-03	+	-	2.4
A_23_P134176	NM_001024465	SOD2	1.0E-04	-	+	3.4
A_24_P217572	NM_001957	EDNRA	2.5E-05	-	+	3.9
A_24_P79403	NM_002619	PF4	1.3E-05	-	+	2.7
A_33_P3290567	NM_003390	WEE1	3.2E-07	-	+	2.6
A_23_P167096	NM_005429	VEGFC	3.4E-02	-	+	3.6
A_23_P23074	NM_006417	IFI44	1.2E-10	-	+	4.6
A_23_P86599	NM_007329	DMBT1	5.0E-04	-	+	2.9
A_24_P146892	NM_032790	ORAI1	5.2E-04	-	+	2.7
A_24_P299685	NM_198389	PDPN	2.9E-02	-	+	3.4
A_32_P108156	NR_001458	MIR155HG	7.2E-05	-	+	4.3
A_33_P3718269	NR_029701	**MIR146A**	3.0E-06	-	+	2.8
A_23_P36611	NM_181861	APAF1	2.9E-07	-	+	2.4
A_33_P3745146	NM_001098517	CADM1	5.9E-08	-	+	2.5
A_23_P300056	NM_044472	CDC42	4.8E-07	-	+	2.5
A_23_P63896	NM_000043	FAS	5.5E-04	-	+	2.7
A_23_P73429	NM_005335	HCLS1	1.4E-05	-	+	2.3
A_33_P3211666	NM_003855	IL18R1	9.9E-03	-	+	2.8
A_23_P60146	NM_006207	PDGFRL	6.1E-03	-	+	2.2
A_23_P401904	NM_001009936	PHF19	2.8E-05	-	+	2.5
A_23_P218770	NM_002872	RAC2	4.2E-05	-	+	2.2
A_23_P406424	NM_175744	RHOC	1.2E-03	-	+	2.3
A_33_P3221748	NM_001031680	RUNX3	8.2E-11	-	+	2.4

Table S3:

Type	Name	Source tissue	Reference
Normal keratinocyte	Oral keratinocyte 17 (**OK17**)	buccal mucosa	[isolated from healthy volunteers]
	Oral keratinocyte 19 (**OK19**)		
	Oral keratinocyte 21 (**OK21**)		
	Oral keratinocyte 23 (**OK23**)		
Immortalized normal keratinocyte	FNB6 hTERT (**FNB6**)		(McGregor *et al*, 2002)
	OKF6/TERT-1 (**OKF6**)	floor of the mouth	(Dickson *et al*, 2000)
Dysplastic	**D4**	tongue	(McGregor *et al*, 2002)
	D6		
	D19		
	D20		
	D35		
HNSCC Metastasis	**TR146**	neck lymph nodes	(Rupniak *et al*, 1985)
	BICR22 (**B22**)		(Edington *et al*, 1995)
HNSCC primary tumour	BICR16 (**B16**)	tongue	
	BICR56 (**B56**)		
	H357		(Prime *et al*, 1990)
	T4	floor of the mouth	(Hunter *et al*, 2006)
	T5	buccal mucosa	

Table S4A: Details of Taqman primers/probes used in the study

Symbol	Gene Name	NCBI Accession #	Assay ID
HOXD10	*Homeobox D10*	NM_002148.3	Hs00157974_m1
B2M	*β-2 microglobulin*	NM_004048.2	Hs00984230_m1
miR-7	*microRNA-7*	NR_029605.1	000386
miR-10b	*microRNA-10b*	NR_029609.1	00218
miR-146a	*microRNA-146a*	NR_029701.1	000468
miR-155	*microRNA-155*	NR_030784.1	002623
RNU48	*small nucleolar RNA, C/D box 48*	NR_002745	001006

Table S4B: Details of SYBR green primers used in the study

Symbol	Gene name	NCBI Accession #	Forward primer (5'→ 3')	Reverse primer (5'→ 3')
ALDH3A1	*aldehyde dehydrogenase 3 family, member A1*	NM_001135168	ACCTGCACAAGAATGAATGGAAC	TCAGGGAGCTTCTGGATCATGTA
ALKBH8	*alkB, alkylation repair homolog 8 (E. coli)*	NM_138775	ATCTGGGGGTCTTCCTGACATT	AATATGAGCGGGAATTCCTTGC
AMOT	*angiomotin*	NM_133265	CATGGAGGGCAGGATTAAGACC	CGACAGCTGCTCTGTCTTGCT
APAF1	*apoptotic peptidase activating factor 1*	NM_181861	TGGAATAACTTCGTATGTAAGGAC	CTTTCAATTTGGAGAGCTTCT
AQP3	*aquaporin 3*	NM_004925	GCTGTATTATGATGCAATCTGGC	CTGTGCCTATGAACTGGTCAAAG
BIRC6	*baculoviral IAP repeat containing 6*	NM_016252	TTTATCATCAGCCTGCCTCATCT	CGTGTTCAGACCAAGGTTCATC
CADM1	*cell adhesion molecule 1*	NM_001098517	TCCTCTACAAGGCTTAACCCGGG	TACCATCACAGGCTGGGGCTT
CD24	*cluster of differentiation 24*	NM_013230	TGCAGAAGAGAGAGTGAGACCAC	AAATCCAACTAATGCCACCACC
CDC42	*cell division cycle 42*	NM_044472	TGTTTGATGAGGCTATCCTAGC	GAAGGGAAGGAGAAAACAGTTTAG
CHST10	*carbohydrate sulfotransferase 10*	NM_004854	TCTAAATGGAGCATTTTCTTCC	ATTTCTGCATCACTGAAGGAA
CLIC3	*chloride intracellular channel 3*	NM_004669	CTGCACATCGTCGACACGGTGTG	CCTGCATCGCGCTGTCCAGGTA
DMBT1	*deleted in malignant brain tumors 1*	NM_007329	ATCTGCTCAGCCACCCAAATAA	AAGCCACCACAATTTGAAGAGG
DNAH5	*dynein, axonemal, heavy chain 5*	NM_001369	ACTAAATACCAGGGCATTGTG	GCAACTCGTTATGAAGGTCAT
EDNRA	*endothelin receptor type A*	NM_001957	GTGTTGACAGGTACAGAGCAGTTGCCTCCT	TCAGGAATGGCCAGGATAAAGGACAGGATC
EYA2	*eyes absent homolog 2 (Drosophila)*	NM_005244	ACCTTCCACACCAGCGAAAGA	CACGAACACACGCTCAATCTCAT
FAS	*Fas (TNF receptor superfamily, member 6)*	NM_000043	TGTTTGGGTGAAGAGAAAGGAA	TGCCACTGTTTCAGGATTTAAAG
FOXA2	*forkhead box A2*	NM_021784	CGTACATGAGCATGTCGGCGGCC	TCATGCCAGCGCCCACGTACG
FOXQ1	*forkhead box Q1*	NM_033260	AAGCAGGGCAGTGACCTGGAGGGC	CTGTTCGCCGTCGCCCTGCGTAT
GBP2	*guanylate binding protein 2, interferon-inducible*	NM_004120	TAAACTTCAGGAACAGGAACG	GAGTATGTTACATATTGGCTCCA
IFI44	*interferon-induced protein 44*	NM_006417	GGGAGTTGGTAAACGCTGGTGTGGTACAT	TGGACTTCCTCTAGCTTGGACCTCACAGG

IGFBP3	*insulin-like growth factor binding protein 3*	NM_001013398	GACAGAATATGGTCCCTGCCGTA	AAGGGCGACACTGCTTTTTCTTA
IL18R1	*interleukin 18 receptor 1*	NM_003855	CAATAGTGGAAGATCGCAGTAAT	CTTACGTTTTTTCCTAATTCCACT
LAMA4	*laminin, alpha 4*	NM_001105206	GCCAAGAACTGTGCAGTGTGCAAC	GCAGTCCATGCCTGTAGGGGG
NANOG	*Nanog homeobox*	NM_024865	CTACAAACAGGTGAAGACCTGG	GTAGGAAGAGTAAAGGCTGGGG
NANOS1	*nanos homolog 1 (Drosophila)*	NM_199461	GAGCTGCAGGTGTGCGTGTTCTG	AGAGCGGGCAGTACTTGATGGTGTG
ORAI1	*ORAI calcium release-activated calcium modulator 1*	NM_032790	GACCACCATCATGGTGCCCTTCGGC	CGCCAGCTCGTTGAGCTCCTGGAAC
PDGFRL	*platelet-derived growth factor receptor-like*	NM_006207	AAGTGGGGACGACATCAGTGTGCTC	TCACAGGCCTTTCATCCTTCTGCCCT
PDPN	*podoplanin*	NM_198389	GGCCGCGGTGCTTTTTAATTT	TTCCCAAAACGAAGAGCAGAGCT
PEBP4	*phosphatidylethanolamine-binding protein 4*	NM_144962	AGGAGTTATCAGCCTACCAGG	GAGAGAGATGACTTTTCCTTCCT
PF4	*platelet factor 4*	NM_002619	CCTCGGTGTCCACTTCAGGCTTCC	CTCAGTGCGATGGGAAACTCGGG
PHF19	*PHD finger protein 19*	NM_001009936	CCCTGCGATGGGTGGATGTGGT	CTGGGGTGCTGGTGAGCTTGCC
PIR	*pirin (iron-binding nuclear protein)*	NM_003662	GAGAACAAGGATCCCAAGAGA	TTCATCACAAATGGACCATGT
PPARGC1A	*peroxisome proliferator-activated receptor gamma, coactivator 1 alpha*	NM_013261	GAAGGCAATTGAAGAGCGCCG	TAGCTGTCTCCATCATCCCGCAG
RAC2	*ras-related C3 botulinum toxin substrate 2 (rho family, small GTP binding protein Rac2)*	NM_002872	CCTGGAGTGCTCAGCTCTCACCCAG	TAGAGGAGGCTGCAGGCGCGCTT
RHOC	*ras homolog gene family, member C*	NM_175744	CCTGACAGCCTGGAAAACATTCCT	GAACGGGCTCCTGCTTCATCTTG
RUNX3	*runt-related transcription factor 3*	NM_001031680	TGACACCGAGCACACCCAGCC	CAGTTCCGAGGTGCCTTGGATTGG
SOD2	*superoxide dismutase 2, mitochondrial*	NM_001024465	CGTTGGCCAAGGGAGATGTTACAGCC	CCAGCAACTCCCCTTTGGGTTCTCC
TF	*transferrin*	NM_001063	CTTGAGAAAGCAGTGGCCAATTTC	CACCCTGGACACAGTTGACACA
TRIM17	*tripartite motif containing 17*	NM_001134855	CACGAGCCCCTCAAGCTTTTCT	CCTCCAGCTTCAACTTGTACCCCT
VEGFC	*vascular endothelial growth factor C*	NM_005429	ACTACCACAGTGTCAGGCAGC	GGAATCCATCTGTTGAGTCATCTC
WEE1	*WEE1 homolog (S. pombe)*	NM_003390	GTAATGGTGGAAGTTTAGCTGAT	CCAAAGACATTGAATGAATATACC
ZNF554	*zinc finger protein 554*	NM_001102651	CTCAAGCCTCCTGTTCAGATTGGATGACT	TGTCCTCTAACTGCTTCCATCCCCCAT
CAV1	*caveolin 1, caveolae protein*	NM_001753	GCAAATACGTAGACTCGGAGGGA	TCAATCTTGACCACGTCATCGTT
HCLS1	*hematopoietic cell-specific Lyn substrate 1*	NM_005335	AAACACGAGTCCCAGAGAGATTATGCCAA	TCATTGAAGCCGACAGCGCTCTTATCCA
JAG2	*jagged 2*	NM_002226	CTCTCTGTGAGGTGGATGTCGACC	ACGGAGCAGTTCTTGCCACCAA
NOTCH1	*notch 1*	NM_017617	CTGCCTGCCAGGCTTCACCGGCCAGAA	TCGGTACAGTACTGACCTGTCCACTCTGG
OCLN	*occludin*	NM_002538	CTGGATCAGGGAATATCCACCTATCA	CAATTCTTTATCCAAACGGGAGAGTTC

Figure legends

Figure 1. HOXD10 expression in a panel of normal, OPL and HNSCC cells and in HNSCC tissues. A HOXD10 expression in a panel of normal oral keratinocytes, oral premaligant lesion and HNSCC cell lines, assessed by qPCR. HOXD10 expression is high in primary HNSCC, low in HNSCC metastases and variable in OPLs. Each assay was conducted in triplicate and repeated 3 times. The data shows the mean of triplicate repeats +/-SEM. **B**. Examples of expression of HOXD10 as assessed by IHC in normal, OPL and HNSCC tissues (from the cohort in C), demonstrating high expression in primary HNSCC. 1 is normal oral mucosa; 2 is OPL, 3 is primary HNSCC and 4 metastatic HNSCC. Photomicrograph overall magnification x200, scale bar=200µm. **C**. Overall IHC Quickscore of HOXD10 expression in the full cohort of tissues from normal mucosa (n=30), OPL (n=18), primary HNSCC (n=82) and HNSCC metastases (n=27). ***p<0.001. **D**. Mean Quickscore of HOXD10 expression assessed by IHC in a panel of 27 matched primary HNSCC with matched metastases. Expression of HOXD10 is lower in the metastasis in 23/27 (85%) of cases (p<0.05).

Figure 2: The effects of over-expression of HOXD10 in low-HOXD10 expressing OPL and HNSCC cells. A. Expression of HOXD10 assessed by qPCR and WB, confirming raised expression in the transfected cells, compared with empty vector transfected controls. B-Actin is used as a loading control in WB. **B-D.** Increasing HOXD10 expression in D19 and B22 increases migration in the transwell assay (B), increases adhesion to fibronectin (C) and increases proliferation as assessed by MTS assay over 96 hours (D). **E**. Increasing HOXD10 expression in D19 and B22 reduces invasion into matrigel. *p<0.05, ***p<0.001. Each assay was conducted in triplicate and repeated 3 times. The data shows the mean of triplicate repeats +/-SEM.

Figure 3: The effects of reduced expression of HOXD10 in high-HOXD10 expressing OPL and HNSCC cells. A. Expression of HOXD10 assessed by qPCR and WB, confirming reduction in expression of HOXD10 in the transfected cells, compared with scrambled siRNA transfected controls. B-Actin is used as a loading control in WB. **B-D.** Reducing HOXD10 expression in D35 and T5 cells reduces migration in the transwell assay (B), reduces adhesion to fibronectin (C) and reduces proliferation as assessed by MTS assay over 96 hours (D). **E**. Reducing HOXD10 expression in D35 and T5 increases invasion into matrigel. *p<0.05, **p<0.01, ***p<0.001. Each assay was conducted in triplicate and repeated 3 times. The data shows the mean of triplicate repeats +/-SEM.

Figure 4: Expression microarray analysis identifies novel putative targets of HOXD10. A. Heat map from the microarray data showing the top 48 differentially expressed genes on manipulation of HOXD10 expression (1 way ANOVA, Benjamini-Hochberg corrected p value <0.05, overall fold change >2). Red= high expression, green = low expression. The full list of these genes can be found in table S1. **B**. Final list of putative HOXD10 targets, filtered by correlation (positive or negative) with HOXD10 expression.

Figure 5: Validation of the microarray data for AMOT-p80 and miR146a and confirmation of direct effect of HOXD10 on expression. A. Expression of AMOT-p80 assessed by qPCR and WB, confirming raised expression in the HOXD10 transfected cells, compared with empty vector transfected controls. B-Actin is used as a loading control. **B.** Expression of AMOT-p80 assessed by qPCR, confirming reduced expression in the HOXD10 siRNA transfected cells, compared with scrambled siRNA controls. **D.** Expression of miR-146a assessed by qPCR, confirming increased expression in the HOXD10 siRNA transfected cells, compared with scrambled siRNA controls. **E**. pGL3 luciferase reporter vectors

containing either WT AMOT promoter, AMOT promoter with either mutated HOXD10 binding sites, or AMOT promoter with both mutated binding sites were transfected into D19 cells stably transfected with either pcDNA3.1-HOXD10 or pcDNA3.1 control plasmids. DLR analysis shows that HOXD10 increases luciferase expression when pGL3 vector contains WT promoter. However, luciferase expression decreases when either of HOXD10 binding sites in AMOT promoter were mutated. No significant reduction in luciferase expression was detected when both mutated sites existed in the same pGL3 vector compared pGL3 vector containing only one mutated binding site. $^{**}p < 0.01$, each assay was conducted in triplicate and repeated 3 times. The data shows the mean of triplicate repeats +/-SEM. **C.** Expression of miR-146a assessed by qPCR, confirming reduced expression in the HOXD10 transfected cells, compared with empty vector transfected controls. **F**. pGL3 luciferase reporter vectors containing either WT miR-146a promoter or miR-146a promoter with a mutated HOXD10 binding site were transfected into D19 cells stably transfected with either pcDNA3.1-HOXD10 or pcDNA3.1 control plasmid. DLR analysis shows that HOXD10 increases luciferase expression when pGL3 vector contains WT promoter. However, luciferase expression decreases when either of HOXD10 binding sites in miR-146a promoter was mutated. $^{**}p < 0.01$, each assay was conducted in triplicate and repeated 3 times. The data shows the mean of triplicate repeats +/-SEM.

Figure 6: AMOT-p80 exerts similar phenotypic effects to that seen on manipulation of HOXD10. A. Expression of AMOT-p80 assessed by qPCR and WB, confirming raised expression of AMOTp80 in transfected cells, compared with empty vector transfected controls. B-Actin is used as a loading control. **B** Cell growth was assessed using the MTS assay over 96 hours. Introducing AMOT into low-AMOT cells (D19, B22) has resulted in an increase in their proliferation. **C**. D19 and B22 cells transfected with AMOT show an increase in migration in the Transwell assay compared to cells transfected with a control plasmid. **D.** Assessing cell adhesion to a fibronectin-coated surface shows that introducing high levels of AMOT by transfection had no significant effect. * $p<0.05$, *** $p<0.001$, each assay was conducted in triplicate and repeated 3 times. The data shows the mean of triplicate repeats +/-SEM.

Figure 7: AMOT-p80 rescues the phenotype seen on knockdown of HOXD10 and is highly expressed in primary HNSCC. **A.** Expression of AMOT assessed by qPCR and WB, confirming reduced expression in the HOXD10 shRNA stably transfected cells, and increased expression in AMOT-p80 transfected cells, compared with empty vector transfected controls. B-Actin is used as a loading control. **B.** Knockdown of HOXD10 expression by siRNA in D19 and B22 increases proliferation as assessed by MTS assay over 96 hours. This is partially rescued by the expression of AMOT in these cells. **C**. Knockdown of HOXD10 expression in D19 and B22 reduces migration in the transwell assay, and this is fully rescued by the over expression of AMOT, to levels higher than controls. **D**. Expression of AMOT as assessed by IHC in normal (1 and 2) and HNSCC tissues (3 and 4), demonstrating high expression in primary HNSCC. Photomicrograph overall magnification x200. * $p<0.05$, **p<0.01, *** $p<0.001$, each assay was conducted in triplicate and repeated 3 times. The data shows the mean of triplicate repeats +/-SEM.

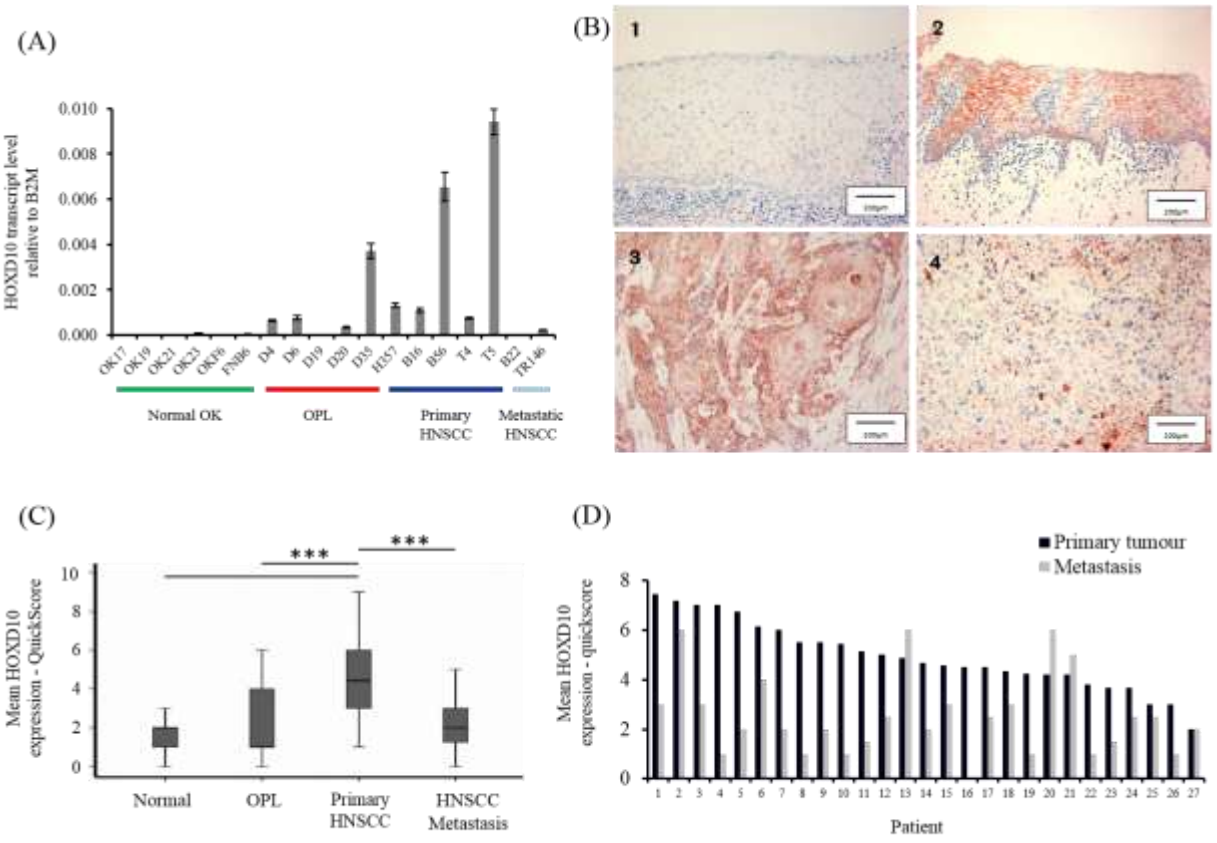

Figure 1.

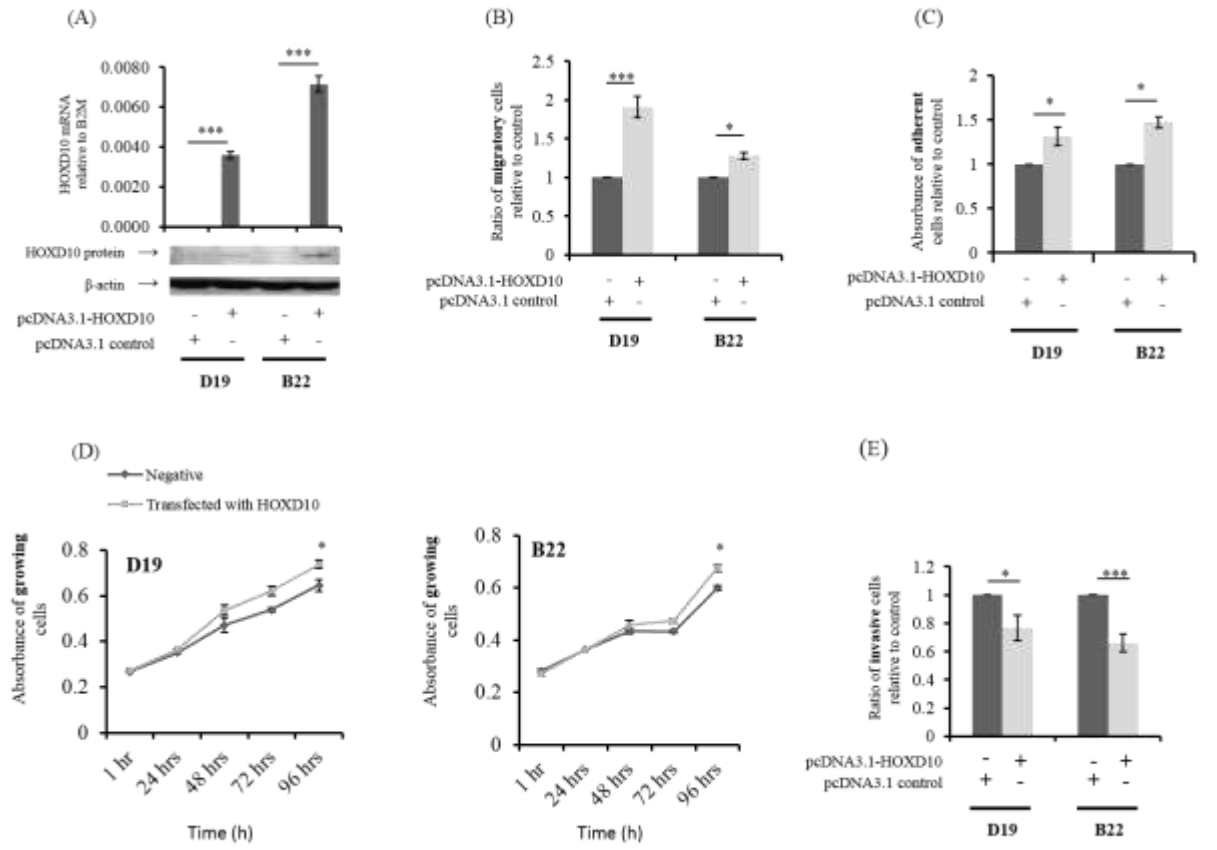

Figure 2.

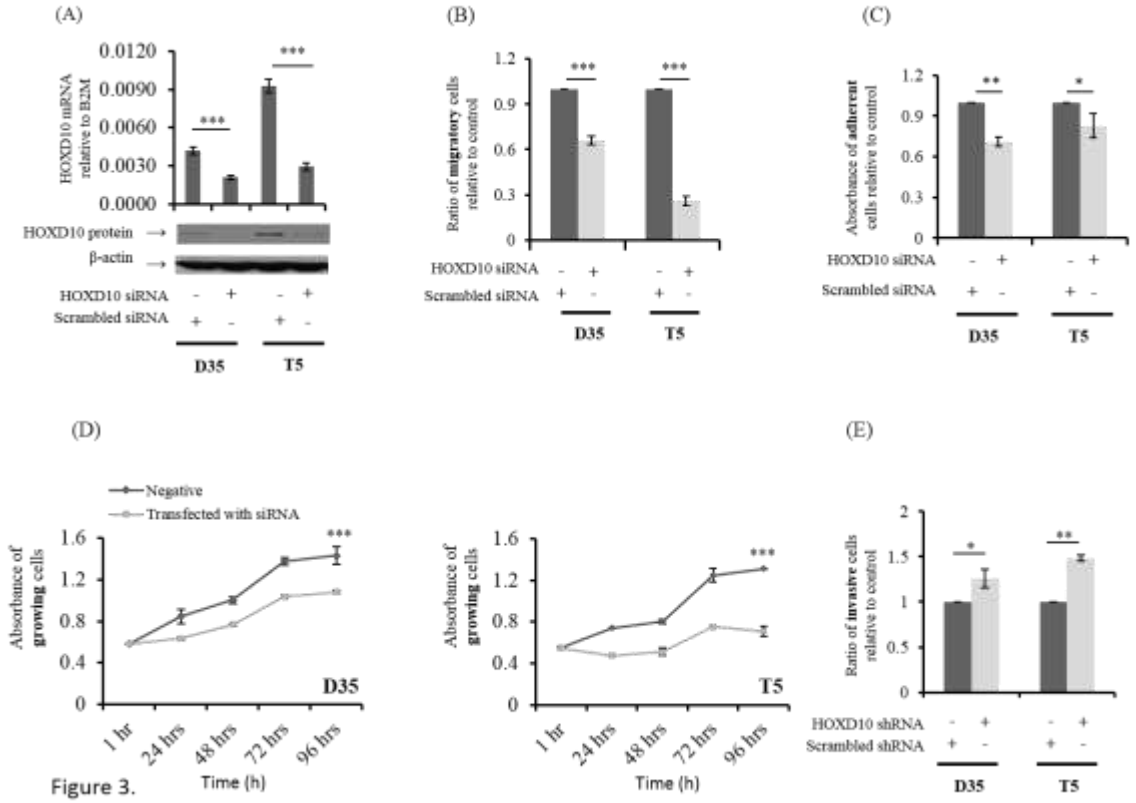

Figure 3.

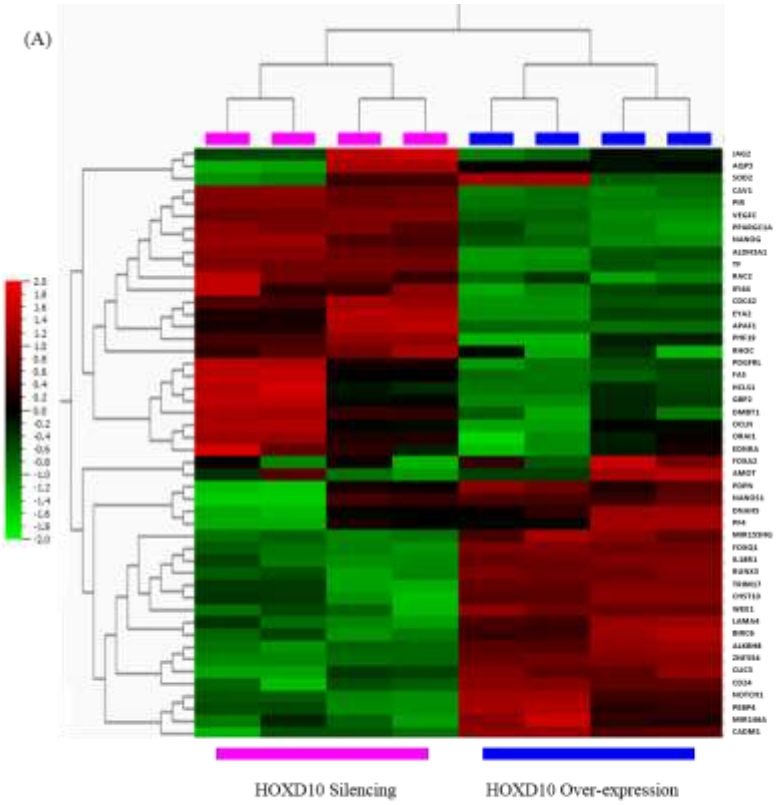

(B)

GENE	Correlation with HOXD10	Examples of reported roles/differential expression
AMOT	+	promotes the proliferation of mammary epithelial cells (8) and regulates endothelial cell migration and linked to angiogenesis (9).
CD24	+	depletion of CD24 reduced cell proliferation, adhesion, and enhanced apoptosis (10) and contributes to tumour growth in urothelial carcinoma (11).
CLIC3	+	elevated in breast cancer in comparison to normal breast tissue and drive cancer progression (12).
AQP3	+	important for growth of oesophageal and oral squamous cell carcinoma (13).
JAG2	+	highly expressed in tongue carcinoma compared to normal tissues (14)
PDGFRL	-	putative tumour suppressor in colorectal cancer cells (15).
miR-155	-	down-regulated in gastric cancer cells and involved in metastasis (16).
miR-146a	-	inhibits cell growth, cell migration and induces apoptosis in non-small cell lung cancer cells (17).

Figure 4.

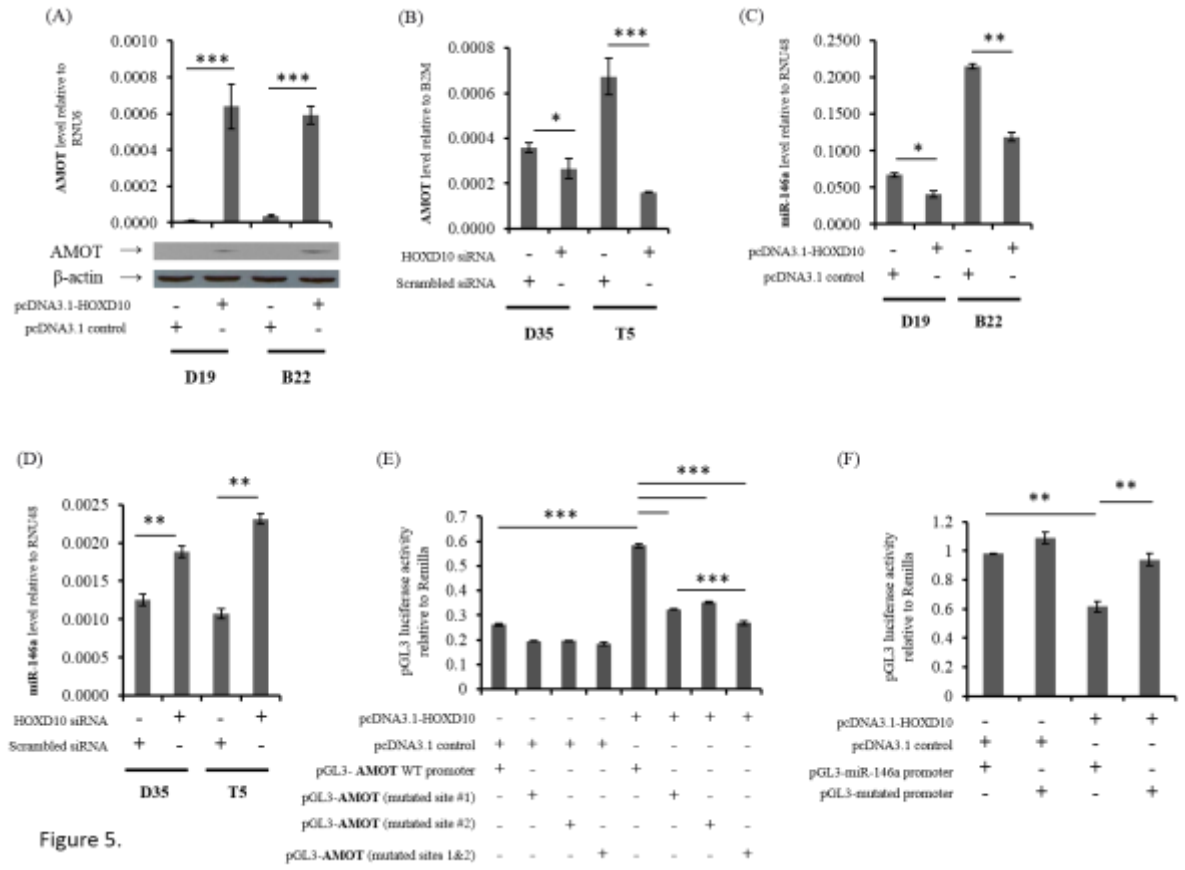

Figure 5.

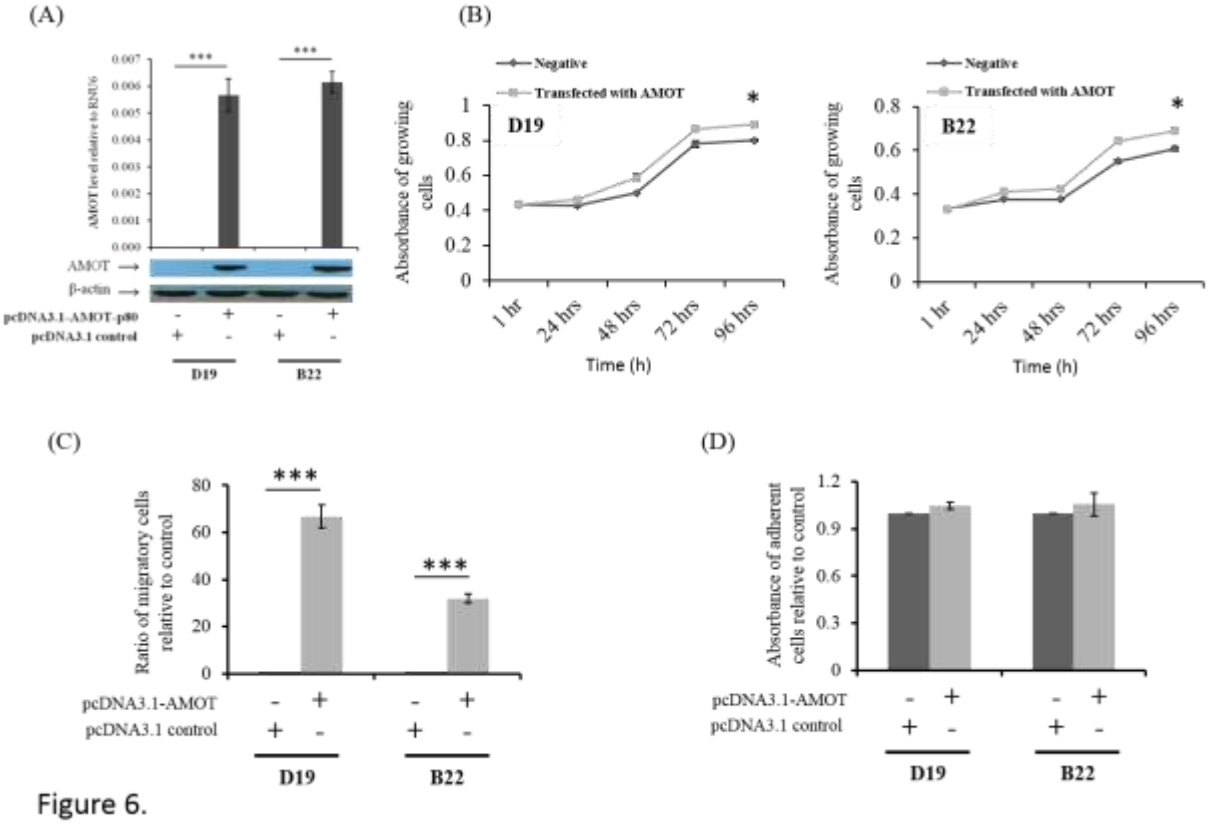

Figure 6.

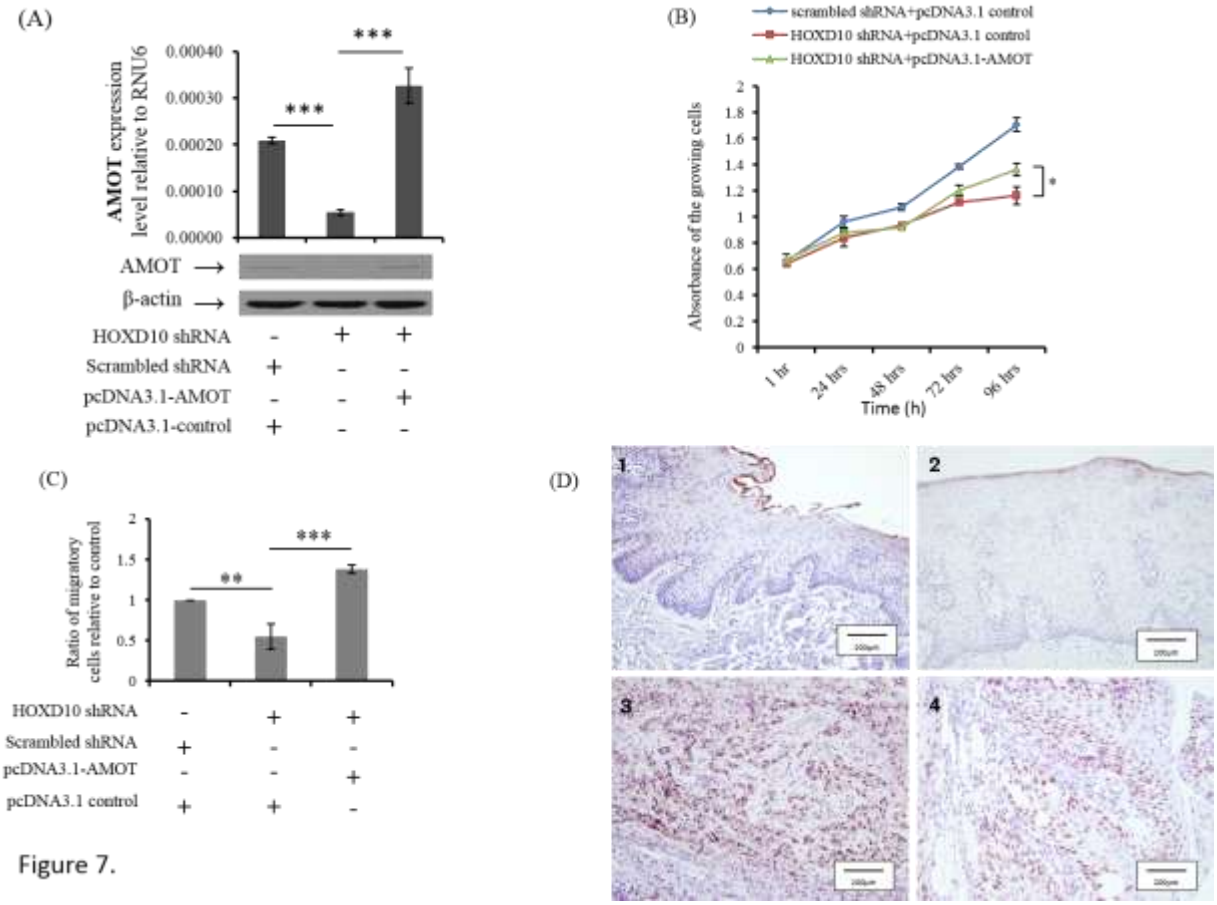
(A)
AMOT expression level relative to RNU6
0.00040
0.00030
0.00020
0.00010
0.00000
***
***
AMOT
β-actin
HOXD10 shRNA - + +
Scrambled shRNA + - -
pcDNA3.1-AMOT - - +
pcDNA3.1-control + - -
(B)
scrambled shRNA+pcDNA3.1 control
HOXD10 shRNA+pcDNA3.1 control
HOXD10 shRNA+pcDNA3.1-AMOT
Absorbance of the growing cells
2
1.8
1.6
1.4
1.2
1
0.8
0.6
0.4
0.2
0
*
1 hr
24 hrs
48 hrs
72 hrs
96 hrs
Time (h)
(C)
Ratio of migratory cells relative to control
2
1.5
1
0.5
0
**
***
HOXD10 shRNA - + +
Scrambled shRNA + - -
pcDNA3.1-AMOT - - +
pcDNA3.1 control + + -
(D)
1
2
3
4

Figure 7.

Supplementary material

Figure S1: Expression of HOXD10 by qPCR and WB in a panel of immortal OPL (D19, D20, and D35) and HNSCC cell lines (B22, H357, B16 and T5) demonstrating close agreement of transcript and protein expression.

Figure S2. Expression of IGFBP3, miR7 and miR10b in an expanded panel of Normal (green), OPL (red) and HNSCC (blue) cells, assessed by qPCR, with HOXD10 expression for comparison.

Figure S3 Percentage of apoptosis cells as measured by Anexin-V-FITC by flow cytometry. Parental and stably transduced HOXD10 overexpression (A and B) or knockdown (C and D) were compared with no consistent change in the percentage of apoptosis cells identified. A small increase in apoptosis was noted in B22 when HOXD10 was overexpressed. * $p<0.05$

Figure S4. Analysis of EMT-associated genes. A: Selected EMT associated genes (as collated from references 15 and 16) which show reciprocal regulation of expression on manipulation of HOXD10. FC (abs) = Absolute fold change. B: Expression of OCLN and JAG2 assessed by qPCR, confirming raised expression in the HOXD10 transfected cells, compared with empty vector transfected controls and confirming reduced expression in the HOXD10 siRNA transfected cells, compared with scrambled siRNA controls. C: Expression of OCLN and JAG2 in an expanded panel of Normal, OPL and HNSCC cells, assessed by qPCR.

Figure S5. Expression of HOXD10 expression (A) for comparison with miR-146a (B) and AMOT-p80 (C) assessed by qPCR in an expanded panel of Normal (green), OPL (red) and HNSCC (blue) cells, assessed by qPCR. WB for AMOT (D) confirms close agreement of transcript and protein levels in the panel of cells.

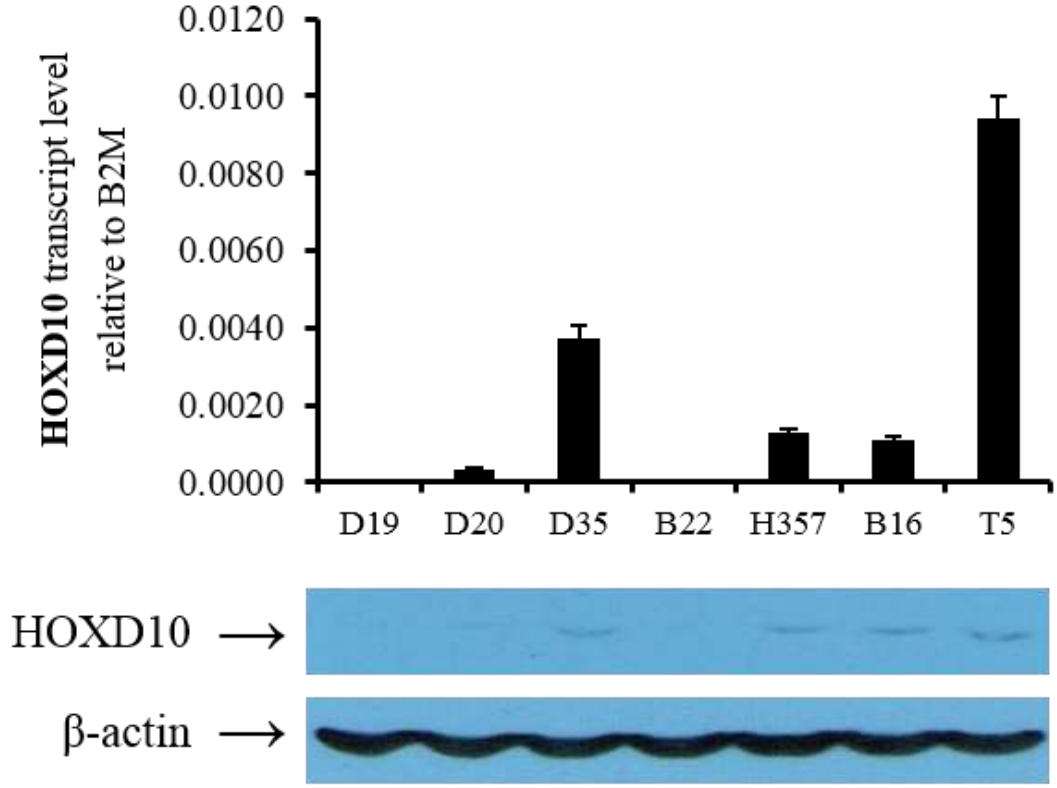
HOXD10 transcript level relative to B2M
0.0120
0.0100
0.0080
0.0060
0.0040
0.0020
0.0000
D19
D20
D35
B22
H357
B16
T5
HOXD10
β-actin

Figure S1.

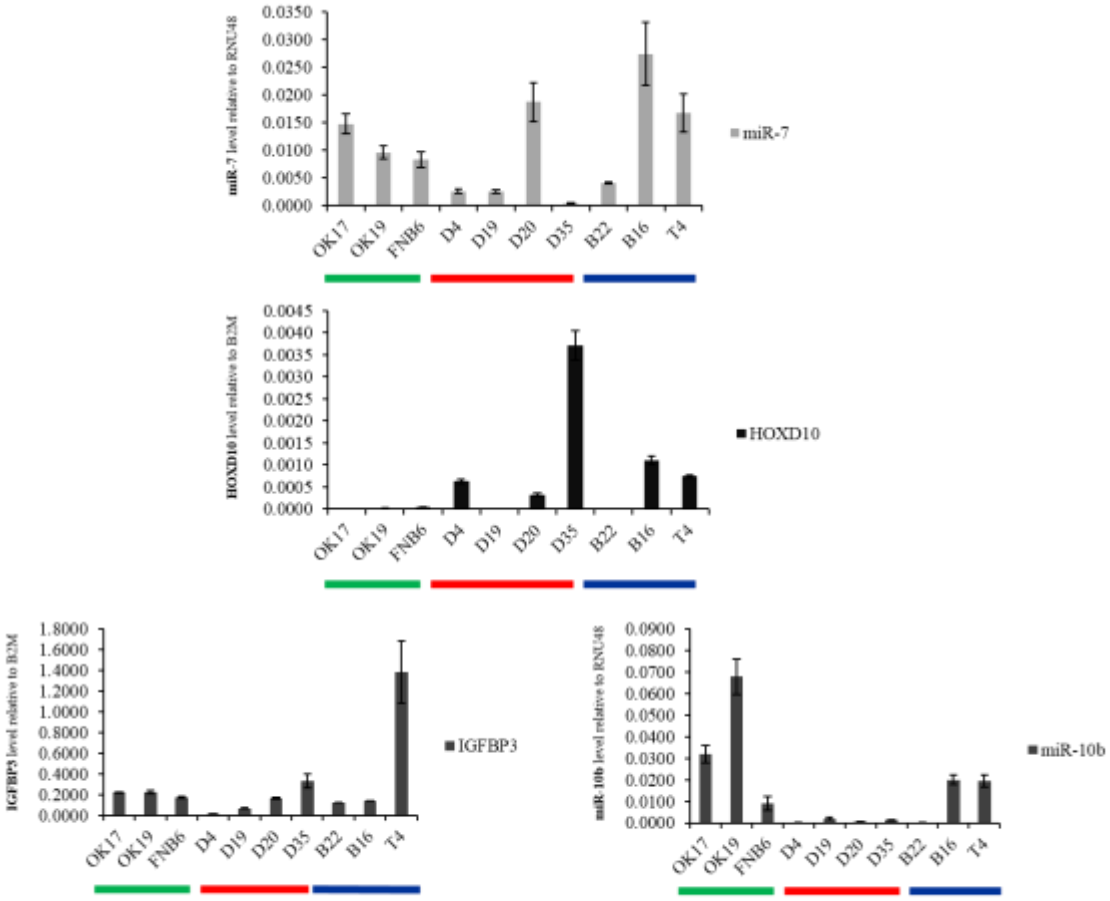

Figure S2.

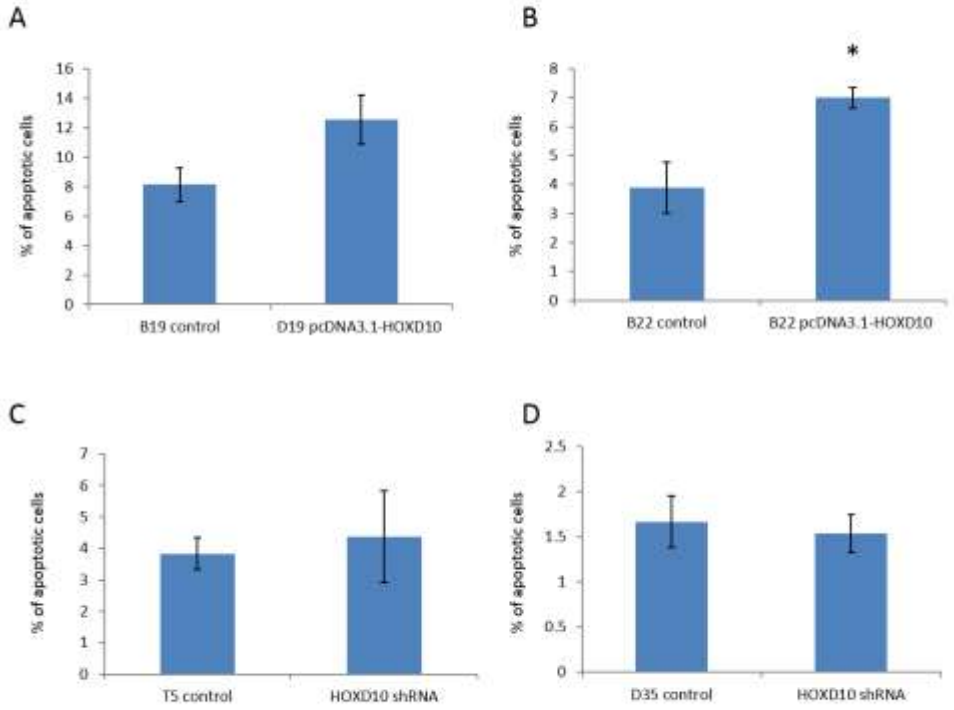

Figure S3

A:

Gene Symbol	HOXD10 Silencing	FC (abs)	HOXD10 Over-expression	FC (abs)
ANTXR2	up	1.7	down	1.1
CYP27B1	up	2.8	down	1.6
IFITM1	up	3.5	down	1.1
IL11	up	5.1	down	1.2
LMCD1	up	1.6	down	1.4
LTBP1	up	1.8	down	1
PRRX1	up	1.1	down	1.6
PTGER2	up	2.3	down	1.1
TIMP3	up	1.5	down	1.3
CA2	down	1.1	up	1.6
HS3ST2	down	1	up	2.7
JAG2	down	1.1	up	1.7
NEFM	down	1	up	2.2
OCLN	down	1.1	up	2.8

B:

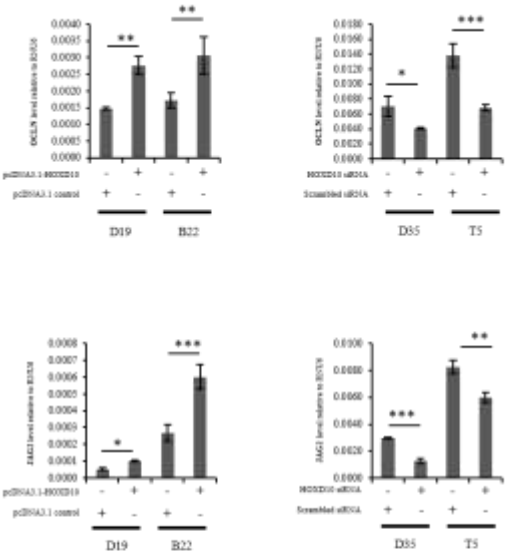

C:

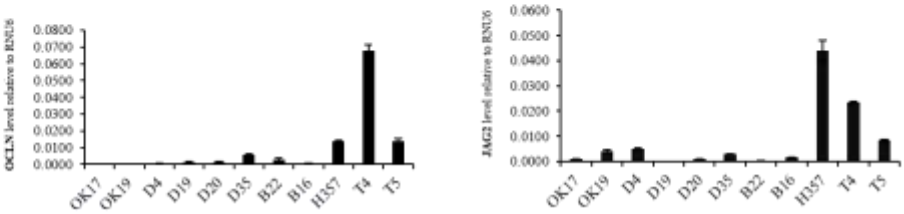

Figure S3.

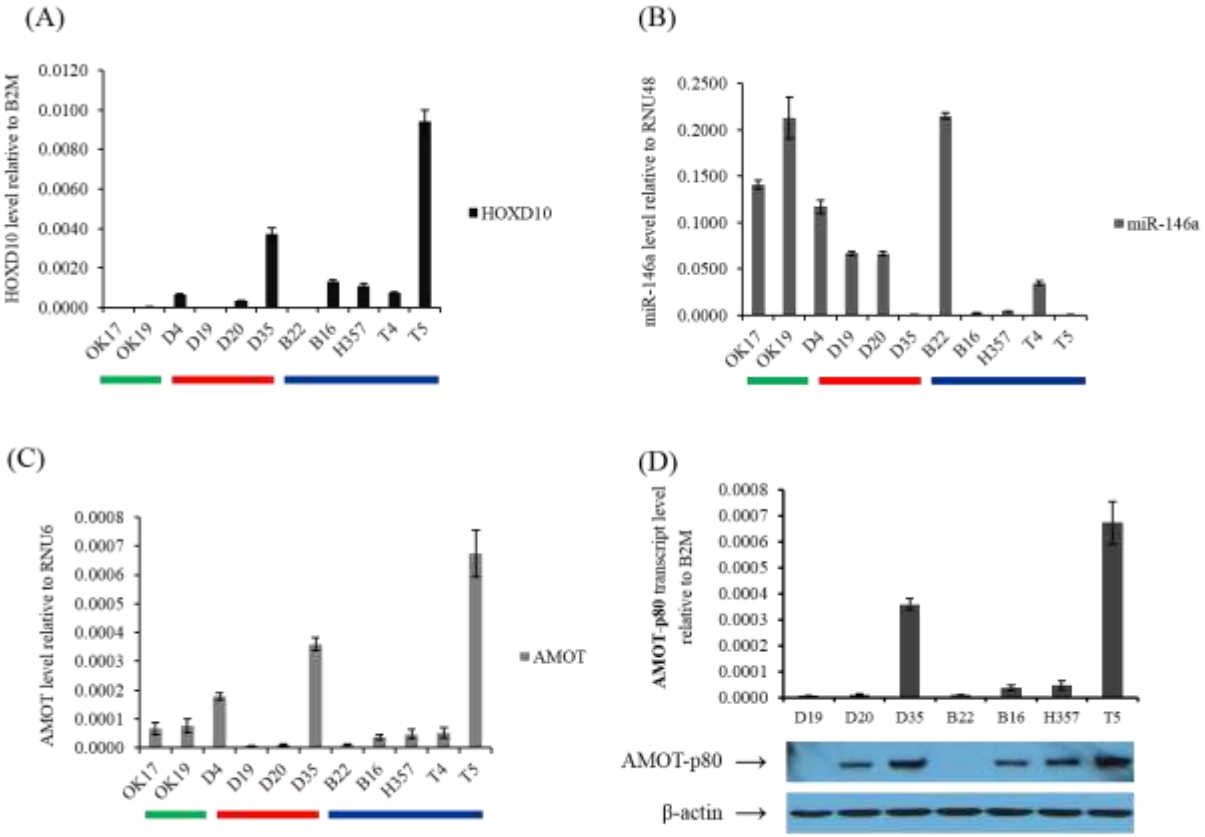

Figure S4.

Table S1. Gene ontology enrichment analysis conducted in DAVID (http://david.abcc.ncifcrf.gov/) demonstrating significantly enriched GO biological processes on manipulation of HOXD10 expression. The total number of significantly differentially expressed genes entered into this analysis was 414.

Table S2. The 48 most significant putative targets of HOXD10.

Table S3. Details of the normal cells and cell lines used in this study. The names given in bold are the abbreviations used in the text.

Table S4. Details of all Taqman and SYBR green primers used in the study

Table S1

Term	Count	%	P Value	Genes	Fold Enrich-ment
GO:0001944~vasculature development	18	4.42	6.58E-05	FGF6, RECK, CAV1, PDPN, PRRX1, ARHGAP24, MMP14, EDNRA, VEGFC, SMO, NOTCH1, LAMA4, APOE, ZC3H12A, AMOT, MKL2, EGF, ANGPTL4	3.12
GO:0030856~regulation of epithelial cell differentiation	6	1.47	4.56E-04	CAV1, NOTCH1, CYP27B1, KRT36, CD24, AQP3	9.03
GO:0048870~cell motility	16	3.93	0.004711	CTHRC1, IL6, PF4, CUZD1, MMP14, DNAH5, SMO, VEGFC, DNER, CATSPER1, AMOT, POU4F1, LHX6, CD24, SCNN1G, AKAP4	2.27
GO:0048589~developmental growth	8	1.97	0.003721	DMBX1, SMO, NOTCH1, ALMS1, IGFBP1, TIMP3, PLAUR, HOXD11	4.01
GO:0042327~positive regulation of phosphorylation	10	2.46	3.70E-04	EDNRA, CSF2, VEGFC, CAV1, IL6, HCLS1, RICTOR, CD24, EGF, IL11	4.50
GO:0043565~sequence-specific DNA binding	23	5.65	0.01489	DMBX1, NANOG, FOXA2, HMBOX1, PRRX1, NR3C2, FOXN2, RORC, HMGA2, VSX1, HOXD10, HOXD11, FOXQ1, NOTCH1, FOXF2, LHX3, PBX1, POU4F1, LHX6, NFE2L3, FOXD1, FOSL1, ETV4	1.72
GO:0050708~regulation of protein secretion	6	1.474201	0.01027	VEGFC, PCSK1, IL6, CADM1, EGF, NLRP3	4.51

Table S2

Probe ID	Accession number	**Gene symbol**	*p* - value (ANOVA)	Effect of HOXD10 over-expression	Effect of HOXD10 silencing	Fold change
A_23_P207213	NM_000691	ALDH3A1	6.2E-04	+	-	4.1
A_23_P212508	NM_001063	TF	6.7E-04	+	-	3.7
A_33_P3322085	NM_001102651	ZNF554	1.4E-03	+	-	5.8
A_33_P3308744	NM_001105206	LAMA4	1.0E-02	+	-	3.1
A_33_P3235078	NM_001134855	TRIM17	4.2E-02	+	-	5.4
A_24_P388786	NM_001369	DNAH5	3.0E-05	+	-	3.3
A_23_P106024	NM_002226	JAG2	6.4E-04	+	-	2.8
A_24_P102053	NM_002538	OCLN	3.8E-02	+	-	3.9
A_23_P85693	NM_004120	GBP2	4.3E-08	+	-	2.9
A_33_P3336686	NM_004669	CLIC3	6.6E-10	+	-	3
A_23_P112482	NM_004925	AQP3	1.8E-03	+	-	3
A_23_P319859	NM_005244	EYA2	1.6E-04	+	-	2.7
A_33_P3369844	NM_013230	CD24	5.5E-04	+	-	3
A_23_P18447	NM_013261	PPARGC1A	5.2E-03	+	-	3.5
A_23_P204640	NM_024865	NANOG	4.2E-03	+	-	2.9
A_32_P164246	NM_033260	FOXQ1	1.8E-06	+	-	3.2
A_24_P344961	NM_133265	**AMOT**	9.0E-07	+	-	3.9
A_24_P383609	NM_199461	NANOS1	1.7E-03	+	-	3
A_33_P3318357	NM_138775	ALKBH8	1.3E-04	+	-	2.7
A_33_P3314902	NM_016252	BIRC6	1.1E-02	+	-	2.2
A_24_P365515	NM_021784	FOXA2	1.9E-02	+	-	2.8
A_23_P134454	NM_001753	CAV1	1.4E-02	+	-	2.3
A_33_P3277198	NM_004854	CHST10	7.0E-06	+	-	2.5
A_33_P3370424	NM_017617	NOTCH1	1.9E-03	+	-	2.1
A_33_P3627001	NM_144962	PEBP4	1.3E-03	+	-	2.3
A_23_P137035	NM_003662	PIR	1.5E-03	+	-	2.4
A_23_P134176	NM_001024465	SOD2	1.0E-04	-	+	3.4
A_24_P217572	NM_001957	EDNRA	2.5E-05	-	+	3.9
A_24_P79403	NM_002619	PF4	1.3E-05	-	+	2.7
A_33_P3290567	NM_003390	WEE1	3.2E-07	-	+	2.6
A_23_P167096	NM_005429	VEGFC	3.4E-02	-	+	3.6
A_23_P23074	NM_006417	IFI44	1.2E-10	-	+	4.6
A_23_P86599	NM_007329	DMBT1	5.0E-04	-	+	2.9
A_24_P146892	NM_032790	ORAI1	5.2E-04	-	+	2.7
A_24_P299685	NM_198389	PDPN	2.9E-02	-	+	3.4
A_32_P108156	NR_001458	MIR155HG	7.2E-05	-	+	4.3
A_33_P3718269	NR_029701	**MIR146A**	3.0E-06	-	+	2.8
A_23_P36611	NM_181861	APAF1	2.9E-07	-	+	2.4
A_33_P3745146	NM_001098517	CADM1	5.9E-08	-	+	2.5
A_23_P300056	NM_044472	CDC42	4.8E-07	-	+	2.5
A_23_P63896	NM_000043	FAS	5.5E-04	-	+	2.7
A_23_P73429	NM_005335	HCLS1	1.4E-05	-	+	2.3
A_33_P3211666	NM_003855	IL18R1	9.9E-03	-	+	2.8
A_23_P60146	NM_006207	PDGFRL	6.1E-03	-	+	2.2
A_23_P401904	NM_001009936	PHF19	2.8E-05	-	+	2.5
A_23_P218770	NM_002872	RAC2	4.2E-05	-	+	2.2
A_23_P406424	NM_175744	RHOC	1.2E-03	-	+	2.3
A_33_P3221748	NM_001031680	RUNX3	8.2E-11	-	+	2.4

Table S3:

Type	Name	Source tissue	Reference
Normal keratinocyte	Oral keratinocyte 17 (**OK17**)	buccal mucosa	[isolated from healthy volunteers]
	Oral keratinocyte 19 (**OK19**)		
	Oral keratinocyte 21 (**OK21**)		
	Oral keratinocyte 23 (**OK23**)		
Immortalized normal keratinocyte	FNB6 hTERT (**FNB6**)		(McGregor *et al*, 2002)
	OKF6/TERT-1 (**OKF6**)	floor of the mouth	(Dickson *et al*, 2000)
Dysplastic	**D4**	tongue	(McGregor *et al*, 2002)
	D6		
	D19		
	D20		
	D35		
HNSCC Metastasis	**TR146**	neck lymph nodes	(Rupniak *et al*, 1985)
	BICR22 (**B22**)		(Edington *et al*, 1995)
HNSCC primary tumour	BICR16 (**B16**)	tongue	
	BICR56 (**B56**)		
	H357		(Prime *et al*, 1990)
	T4	floor of the mouth	(Hunter *et al*, 2006)
	T5	buccal mucosa	

Table S4A: Details of Taqman primers/probes used in the study

Symbol	Gene Name	NCBI Accession #	Assay ID
HOXD10	*Homeobox D10*	NM_002148.3	Hs00157974_m1
B2M	*β-2 microglobulin*	NM_004048.2	Hs00984230_m1
miR-7	*microRNA-7*	NR_029605.1	000386
miR-10b	*microRNA-10b*	NR_029609.1	00218
miR-146a	*microRNA-146a*	NR_029701.1	000468
miR-155	*microRNA-155*	NR_030784.1	002623
RNU48	*small nucleolar RNA, C/D box 48*	NR_002745	001006

Table S4B: Details of SYBR green primers used in the study

Symbol	Gene name	NCBI Accession #	Forward primer (5'→ 3')	Reverse primer (5'→ 3')
ALDH3A1	*aldehyde dehydrogenase 3 family, member A1*	NM_001135168	ACCTGCACAAGAATGAATGGAAC	TCAGGGAGCTTCTGGATCATGTA
ALKBH8	*alkB, alkylation repair homolog 8 (E. coli)*	NM_138775	ATCTGGGGGTCTTCCTGACATT	AATATGAGCGGGAATTCCTTGC
AMOT	*angiomotin*	NM_133265	CATGGAGGGCAGGATTAAGACC	CGACAGCTGCTCTGTCTTGCT
APAF1	*apoptotic peptidase activating factor 1*	NM_181861	TGGAATAACTTCGTATGTAAGGAC	CTTTCAATTTGGAGAGCTTCT
AQP3	*aquaporin 3*	NM_004925	GCTGTATTATGATGCAATCTGGC	CTGTGCCTATGAACTGGTCAAAG
BIRC6	*baculoviral IAP repeat containing 6*	NM_016252	TTTATCATCAGCCTGCCTCATCT	CGTGTTCAGACCAAGGTTCATC
CADM1	*cell adhesion molecule 1*	NM_001098517	TCCTCTACAAGGCTTAACCCGGG	TACCATCACAGGCTGGGGCTT
CD24	*cluster of differentiation 24*	NM_013230	TGCAGAAGAGAGAGTGAGACCAC	AAATCCAACTAATGCCACCACC
CDC42	*cell division cycle 42*	NM_044472	TGTTTGATGAGGCTATCCTAGC	GAAGGGAAGGAGAAAACAGTTTAG
CHST10	*carbohydrate sulfotransferase 10*	NM_004854	TCTAAATGGAGCATTTTCTTCC	ATTTCTGCATCACTGAAGGAA
CLIC3	*chloride intracellular channel 3*	NM_004669	CTGCACATCGTCGACACGGTGTG	CCTGCATCGCGCTGTCCAGGTA
DMBT1	*deleted in malignant brain tumors 1*	NM_007329	ATCTGCTCAGCCACCCAAATAA	AAGCCACCACAATTTGAAGAGG
DNAH5	*dynein, axonemal, heavy chain 5*	NM_001369	ACTAAATACCAGGGCATTGTG	GCAACTCGTTATGAAGGTCAT
EDNRA	*endothelin receptor type A*	NM_001957	GTGTTGACAGGTACAGAGCAGTTGCCTCCT	TCAGGAATGGCCAGGATAAAGGACAGGATC
EYA2	*eyes absent homolog 2 (Drosophila)*	NM_005244	ACCTTCCACACCAGCGAAAGA	CACGAACACACGCTCAATCTCAT
FAS	*Fas (TNF receptor superfamily, member 6)*	NM_000043	TGTTTGGGTGAAGAGAAAGGAA	TGCCACTGTTTCAGGATTTAAAG
FOXA2	*forkhead box A2*	NM_021784	CGTACATGAGCATGTCGGCGGCC	TCATGCCAGCGCCCACGTACG
FOXQ1	*forkhead box Q1*	NM_033260	AAGCAGGGCAGTGACCTGGAGGGC	CTGTTCGCCGTCGCCCTGCGTAT
GBP2	*guanylate binding protein 2,*	NM_004120	TAAACTTCAGGAACAGGAACG	GAGTATGTTACATATTGGCTCC

	interferon-inducible			A
IFI44	*interferon-induced protein 44*	NM_006417	GGGAGTTGGTAAACGCTGGTG TGGTACAT	TGGACTTCCTCTAGCTTGGACCT CACAGG
IGFBP3	*insulin-like growth factor binding protein 3*	NM_001013398	GACAGAATATGGTCCCTGCCGT A	AAGGGCGACACTGCTTTTTCTT A
IL18R1	*interleukin 18 receptor 1*	NM_003855	CAATAGTGGAAGATCGCAGTA AT	CTTACGTTTTTTCCTAATTCCAC T
LAMA4	*laminin, alpha 4*	NM_001105206	GCCAAGAACTGTGCAGTGTGCA AC	GCAGTCCATGCCTGTAGGGGG
NANOG	*Nanog homeobox*	NM_024865	CTACAAACAGGTGAAGACCTG G	GTAGGAAGAGTAAAGGCTGGG G
NANOS1	*nanos homolog 1 (Drosophila)*	NM_199461	GAGCTGCAGGTGTGCGTGTTCT G	AGAGCGGGCAGTACTTGATGG TGTG
ORAI1	*ORAI calcium release-activated calcium modulator 1*	NM_032790	GACCACCATCATGGTGCCCTTC GGC	CGCCAGCTCGTTGAGCTCCTGG AAC
PDGFRL	*platelet-derived growth factor receptor-like*	NM_006207	AAGTGGGGACGACATCAGTGT GCTC	TCACAGGCCTTTCATCCTTCTGC CCT
PDPN	*podoplanin*	NM_198389	GGCCGCGGTGCTTTTTAATTT	TTCCCAAAACGAAGAGCAGAG CT
PEBP4	*phosphatidylethanolamine-binding protein 4*	NM_144962	AGGAGTTATCAGCCTACCAGG	GAGAGAGATGACTTTTCCTTCC T
PF4	*platelet factor 4*	NM_002619	CCTCGGTGTCCACTTCAGGCTTC C	CTCAGTGCGATGGGAAACTCG GG
PHF19	*PHD finger protein 19*	NM_001009936	CCCTGCGATGGGTGGATGTGGT	CTGGGGTGCTGGTGAGCTTGCC
PIR	*pirin (iron-binding nuclear protein)*	NM_003662	GAGAACAAGGATCCCAAGAGA	TTCATCACAAATGGACCATGT
PPARGC1A	*peroxisome proliferator-activated receptor gamma, coactivator 1 alpha*	NM_013261	GAAGGCAATTGAAGAGCGCCG	TAGCTGTCTCCATCATCCCGCA G
RAC2	*ras-related C3 botulinum toxin substrate 2 (rho family, small GTP binding protein Rac2)*	NM_002872	CCTGGAGTGCTCAGCTCTCACC CAG	TAGAGGAGGCTGCAGGCGCGC TT
RHOC	*ras homolog gene family, member C*	NM_175744	CCTGACAGCCTGGAAAACATTC CT	GAACGGGCTCCTGCTTCATCTT G
RUNX3	*runt-related transcription factor 3*	NM_001031680	TGACACCGAGCACACCCAGCC	CAGTTCCGAGGTGCCTTGGATT GG
SOD2	*superoxide dismutase 2, mitochondrial*	NM_001024465	CGTTGGCCAAGGGAGATGTTAC AGCC	CCAGCAACTCCCCTTTGGGTTCT CC
TF	*transferrin*	NM_001063	CTTGAGAAAGCAGTGGCCAATT TC	CACCCTGGACACAGTTGACACA
TRIM17	*tripartite motif containing 17*	NM_001134855	CACGAGCCCCTCAAGCTTTTCT	CCTCCAGCTTCAACTTGTACCCC T
VEGFC	*vascular endothelial growth factor C*	NM_005429	ACTACCACAGTGTCAGGCAGC	GGAATCCATCTGTTGAGTCATC TC
WEE1	*WEE1 homolog (S. pombe)*	NM_003390	GTAATGGTGGAAGTTTAGCTGA T	CCAAAGACATTGAATGAATATA CC
ZNF554	*zinc finger protein 554*	NM_001102651	CTCAAGCCTCCTGTTCAGATTG GATGACT	TGTCCTCTAACTGCTTCCATCCC CCAT
CAV1	*caveolin 1, caveolae protein*	NM_001753	GCAAATACGTAGACTCGGAGG GA	TCAATCTTGACCACGTCATCGTT
HCLS1	*hematopoietic cell-specific Lyn substrate 1*	NM_005335	AAACACGAGTCCCAGAGAGATT ATGCCAA	TCATTGAAGCCGACAGCGCTCT TATCCA
JAG2	*jagged 2*	NM_002226	CTCTCTGTGAGGTGGATGTCGA CC	ACGGAGCAGTTCTTGCCACCAA
NOTCH1	*notch 1*	NM_017617	CTGCCTGCCAGGCTTCACCGGC CAGAA	TCGGTACAGTACTGACCTGTCC ACTCTGG
OCLN	*occludin*	NM_002538	CTGGATCAGGGAATATCCACCT ATCA	CAATTCTTTATCCAAACGGGAG AGTTC